WL-TR-95 -3038

FLUTTER CONTROL OF AN ADAPTIVE LAMINATED COMPOSITE PANEL WITH PIEZOELECTRIC LAYERS

AFZALSULEMAN
VIPPERLA B. VENKAYYA

Design Methods Development Section
Design Development Branch
Structures Division

August 1994

FINAL REPORT FOR PERIOD SEPTEMBER 1992 - AUGUST 1994

DTIC
ELECTE
MAY 24 1995
S D
B

Approved for public release; distribution is unlimited.

FLIGHT DYNAMICS DIRECTORATE
WRIGHT LABORATORY
AIR FORCE MATERIEL COMMAND
WRIGHT PATTERSON AFB OH 45433-7542

19950522 021

DTIC QUALITY INSPECTED 1

NOTICE

When Government drawings, specifications, or other data are used for any purpose other than in connection with a definitely related Government procurement operation, the United States Government thereby incurs no responsibility or any obligation whatsoever. The fact that the Government may have formulated or in any way supplied the said drawings, specifications, or other data, is not to be regarded by implication, or otherwise as in any manner, as licensing the holder or any other person or corporation; or as conveying any rights or permission to manufacture, use, or sell any patented invention that may in any way be related thereto.

This report is releasable to the National Technical Information Service (NTIS). At NTIS, it will be available to the general public, including foreign nations.

This technical report has been reviewed and is approved for publication.

VIPPERLA B. VENKAYYA, Principal Scientist
Design Methods Development Section
Design Development Branch

NELSON D. WOLF, Technical Manager
Design Methods Development Section
Design Development Branch

GEORGE R. HOLDERBY, Chief
Design Development Branch
Structures Division

"If your address has changed, if you wish to be removed from our mailing list, or if the addressee is no longer employed by your organization please notify WL/FIBAD, Wright-Patterson AFB OH 45433-7542 to help us maintain a current mailing list".

Copies of this report should not be returned unless return is required by security considerations, contractual obligations, or notice on a specific document.

DISCLAIMER NOTICE

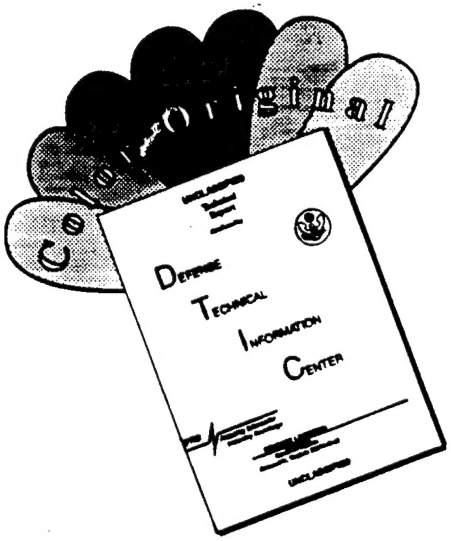

THIS DOCUMENT IS BEST QUALITY AVAILABLE. THE COPY FURNISHED TO DTIC CONTAINED A SIGNIFICANT NUMBER OF COLOR PAGES WHICH DO NOT REPRODUCE LEGIBLY ON BLACK AND WHITE MICROFICHE.

REPORT DOCUMENTATION PAGE

Form Approved
OMB No. 0704-0188

Public reporting burden for this collection of information is estimated to average 1 hour per response, including the time for reviewing instructions, searching existing data sources, gathering and maintaining the data needed, and completing and reviewing the collection of information. Send comments regarding this burden estimate or any other aspect of this collection of information, including suggestions for reducing this burden, to Washington Headquarters Services, Directorate for Information Operations and Reports, 1215 Jefferson Davis Highway, Suite 1204, Arlington, VA 22202-4302, and to the Office of Management and Budget, Paperwork Reduction Project (0704-0188), Washington, DC 20503.

1. AGENCY USE ONLY *(Leave blank)*	2. REPORT DATE	3. REPORT TYPE AND DATES COVERED
	August 1994	Final Report, 1 September 1992 - 31 August

4. TITLE AND SUBTITLE
Flutter Control of an Adaptive Laminated Composite Panel with Piezoelectric Layers

5. FUNDING NUMBERS
NRC/AFOSR
PE: 61102

6. AUTHOR(S)
Afzal Suleman and Vipperla B. Venkayya

7. PERFORMING ORGANIZATION NAME(S) AND ADDRESS(ES)
NRC/AFOSR
Research Associateship Programs
2101 Constitution Ave.
Washington DC

8. PERFORMING ORGANIZATION REPORT NUMBER

9. SPONSORING/MONITORING AGENCY NAME(S) AND ADDRESS(ES)
Flight Dynamics Directorate
Wright Laboratory
Air Force Materiel Command
Wright Patterson AFB OH 45433-7542

10. SPONSORING/MONITORING AGENCY REPORT NUMBER
WL-TR-95-3038

11. SUPPLEMENTARY NOTES

12a. DISTRIBUTION/AVAILABILITY STATEMENT
Approved for public release; Distribution unlimited.

12b. DISTRIBUTION CODE

13. ABSTRACT *(Maximum 200 words)*

A new finite element formulation of an adaptive composite laminated panel with piezoelectric sensors and actuators is presented. Classical laminated theory with electromechanical induced actuation and variational principles are used to formulate the equations of motion. The finite element model based on the bilinear Mindlin plate theory with 24 structural degrees of freedom and one electrical degree of freedom per piezoelectric layer is much simpler and computationally more efficient than models based on solid element formulations with a significant decrease in the number of degrees of freedom. The numerical results from simulations agree well with data reported in the literature.

Next, the effectiveness of using the adaptive composite panel to control panel flutter is examined. First order piston theory is used to model the supersonic flow. The piezoelectric actuators are used passively to induce inplane forces to alter the panel stiffness characteristics. The results show that piezoelectric devices can significantly increase panel flutter velocities. However, it was found that the added mass to stiffness ratio and the piezoelectric patch configuration are two factors affecting actuator performance.

14. SUBJECT TERMS
Finite Element Analysis, Piezoelectric Actuation and Sensing, Panel Flutter, Passive Control

15. NUMBER OF PAGES
76

16. PRICE CODE

17. SECURITY CLASSIFICATION OF REPORT	18. SECURITY CLASSIFICATION OF THIS PAGE	19. SECURITY CLASSIFICATION OF ABSTRACT	20. LIMITATION OF ABSTRACT
Unclassified	Unclassified	Unclassified	Unlimited

NSN 7540-01-280-5500

Standard Form 298 (Rev. 2-89)
Prescribed by ANSI Std. Z39-18

CONTENTS

ABSTRACT v
FOREWORD vi
LIST OF FIGURES vii
LIST OF TABLES ix

1. INTRODUCTION 1
   1.1 ENABLING TECHNOLOGIES 2
      1.1.1 Materials 3
      1.1.2 Actuators 5
      1.1.3 Sensors 7
      1.1.4 Control Design and Optimization 8
   1.2 APPLICATIONS 10
   1.3 PRESENT INVESTIGATION 13

2. ELECTROMECHANICAL FINITE ELEMENT 15
   2.1 FINITE ELEMENT FORMULATION 16
      2.1.1 Mindlin Plate Theory 16
      2.1.2 Electromechanical Plate Finite Element 18
      2.1.3 Constitutive Relations 20
      2.1.4 Strain-Displacement Relations 21
      2.1.5 Stress-Strain Relations 22
   2.2 EQUATIONS OF MOTION 24
   2.3 SIMULATION RESULTS 24
      2.3.1 Static Actuation and Sensing 25
      2.3.2 Eigenvalue Solution 27
   2.4 COMMERCIAL FEM CODES 36
      2.4.1 ANSYS - Swanson Analysis Systems, Inc. 36
      2.4.2 ABAQUS - Hibbit, Karlsson & Sorensen, Inc. 36
      2.4.3 NASTRAN(CSA) - CSAR Corporation 37
      2.4.4 NASTRAN(MSC) - The MacNeal-Schwendler Corp. . . 39
      2.4.5 Simulation Results 39

2.5 THERMAL ANALOGY 40
2.6 PRELIMINARY REMARKS 41

3. APPLICATION - FLUTTER CONTROL 43
3.1 DESIGN PROBLEM 43
3.2 PANEL FLUTTER MODEL 46
3.2.1 First Order Piston Theory 46
3.2.2 The Effect of Initial Pre-Stresses 48
3.2.3 Equations of Motion 49
3.3 PASSIVE CONTROL 50
3.4 PRELIMINARY REMARKS 54

4. CONCLUDING REMARKS 56
REFERENCES 58

APPENDICES
A PROGRAM INPUT DATA 62
B POST-PROCESSING PROGRAM 67

FOREWORD

This technical report was prepared by Dr. Afzal Suleman and Dr. Vipperla B. Venkayya, Design Development Branch, Structures Division of the Flight Dynamics Directorate. This effort was supported by the National Research Council (NRC) and the Air Force Office for Scientific Research (AFOSR). This technical report covers the work accomplished between September 1992 and August 1994.

Accession For
NTIS GRA&I ☑
DTIC TAB ☐
Unannounced ☐
Justification
By
Distribution/
Availability Codes
Dist | Avail and/or Special
A-1

LIST OF FIGURES

Figure 1.1 Key technologies and fields that need to be addressed in order to enable adaptation in structural systems.

Figure 1.2 Application of adaptive structures technology to aeronautical systems.

Figure 2.1 Finite element composite plate element showing the displacement degrees of freedom for the mechanical elastic properties and the electrical degrees of freedom for the piezoelectric behaviour.

Figure 2.2 Piezoelectric patch showing direction of polarization and electrode layout.

Figure 2.3 (a) Test study comparison between the present formulation and Tzou and Tseng (1990) showing the experimental apparatus for the piezoelectric bimorph plate; (b) the finite element model with 53 degrees of freedom; (c) the static actuation mechanism; (d) the static sensing mechanism.

Figure 2.4 (a) The experimental apparatus showing the Gr/Epoxy [0/±45] cantilevered plate studied by Crawley and Lazarus (1991); (b) The finite element model with 880 degrees of freedom; (c) the static actuation mechanism; (d) the deformed configuration of the cantilevered plate resulting from the static actuation for an applied voltage of $\pm 158V$; (e) comparison of the sensing voltages along the central tier of piezoelectric elements due to voltage of $\pm 100V$ applied on the outer tiers of piezoelectrics; and (e) the deformed configuration showing the sensed voltages along the central tier of piezoelectrics.

Figure 2.5 Comparison between the present formulation and Ha, Keilers and

Chang (1992) showing: (a) the relationship between the required actuation voltages and the various tip loading conditions; (b) The deformed configuration of the cantilevered plate under the action of the mechanical tip load and electric actuation.

Figure 2.6 Eigenvalue solution comparison between the present formulation and Hollkamp (1994) showing: (a) the experimental apparatus for the aluminum cantilever beam with 6 pairs of PZT tiles; and (b) the finite element model with 195 degrees of freedom.

Figure 2-7 Comparison between the solid element models developed in ANSYS and ABAQUS and the composite plate element developed here.

Figure 2-8 An example to establish the analogy between the thermal and piezoelectric behaviour.

Figure 3.1 Self excited oscillations of an external panel of a flight vehicle exposed to supersonic air flow ($M > \sqrt{2}$)

Figure 3.2 Effect of in-plane tensile forces.

Figure 3.3 Initial in-plane pre-stresses on the panel due to piezoelectric actuation.

Figure 3.4 The natural frequencies solution as a function of dynamic pressure. The fundamental mode shapes are shown in vacuum and following the onset of flutter.

Figure 3.5 Critical dynamic pressure results for a central piezoelectric patch configuration for two sizes of actuation capabilities.

Figure 3.6 Critical dynamic pressure results for three different patch configurations.

LIST OF TABLES

Table 2-1 Input data card deck for ANSYS showing the necessary commands to perform a piezoelectric analysis.

Table 2-2 Input data card deck for ABAQUS showing the necessary commands to perform a piezoelectric analysis.

Table 3-1 Material properties and operating conditions for a G1195 PZT piezoceramic.

Table 3-2 The actuation capabilities and power requirements for a typical piezoceramic patch.

Table 3-3 Passive control methodology flowchart.

CHAPTER
ONE

INTRODUCTION

In the past decade, technological developments in materials and computer sciences have evolved to the point where their synergistic combination have culminated in a new field of multi-disciplinary research in adaptation. The advances in material sciences have provided a comprehensive and theoretical framework for implementing multifunctionality into materials, and the development of high speed digital computers has permitted the transformation of that framework into methodologies for practical design and production. The concept is elementary: a highly integrated sensor system provides data on the structures environment to a processing and control system which in turn signals integrated actuators to modify the structural properties in an appropriate fashion.

U.S.A., Japan and Europe have been interested for some time in applying the adaptation concept to high performance aircraft, high pointing accuracy space systems and variable geometry manipulators.

In the USA, studies at MIT (Lazarus, Crawley and Bohlman, 1990) have investigated the properties of composite laminates with embedded piezoelectric actuators. Work performed at VPI (Anders and Rogers, 1990) has proposed fiber optic sensors embedded in composite materials for sensing and shape memory alloys for actuation of structures. Adaptive structure concepts for vibration suppression are being developed at JPL as well (Wada, 1991). Activities here focus on the development of concepts, integrated design methodology and ground test methodology including

the development of passive and active structural members. Since then numerous other investigators have proposed the application of adaptive technologies to structural systems, and various workshops, conferences (e.g. International Conference on Adaptive Structures) and journals (e.g. Journal of Intelligent Materials, Systems and Structures) have been organized to provide a forum for discussion on these matters.

Most of the work undertaken in Japan (Miura and Natori, 1991) has concentrated on adaptive truss structures. In the early eighties, researchers at ISAS proposed a coilable longeron mast concept to efficiently package space truss structures with capabilities to adapt its geometry to mission requirements. Subsequently, extensive research has been carried out in the areas of vibration suppression and shape control, with particular application to space structures.

European activities include the work on shape memory alloys at the University of Twente in the Netherlands and piezoceramics at ONERA in France. Potential space applications for adaptive structures are also being explored at ESA (Breitbach, 1991). Recently, the Smart Structures Research Institute at Strathclyde University in Scotland has also been established (Gardiner et al., 1991)

1.1 ENABLING TECHNOLOGIES

There are two key technological developments which have combined to establish the potential feasibility of adaptive structures. The first is the development of functional materials (materials science) and their utilization in devices such as distributed actuators and sensors (mechanical engineering). The second development comes in the electrical engineering field, with new control algorithms and signal processing technologies. Figure 1 depicts technologies and other research fields which need to be addressed to enable the implementation of adaptive materials into structural systems.

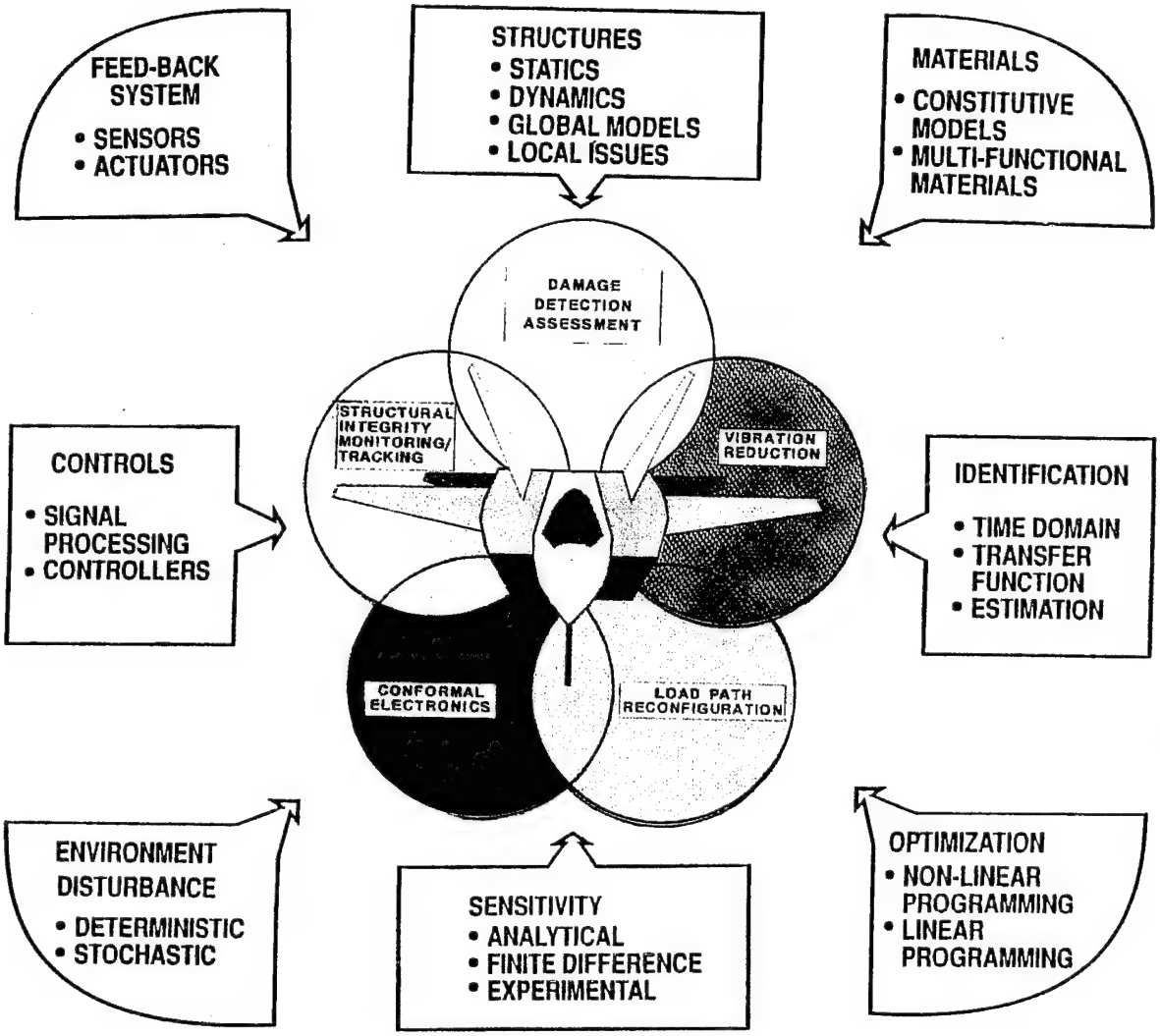

Figure 1.1 Key technologies and fields that need to be addressed in order to enable adaptation in structural systems.

1.1.1 Materials

Materials science has shown a distinct trend in the development of materials with functional properties. There are five types of adaptive materials that have been widely reported in the literature: piezoelectrics, shape memory alloys, electrostrictors, magnetostrictors and electro-rheological fluids.

Piezoelectric materials currently come in the form of piezoceramics and piezopolymers. Piezoceramics are polycrystalline ceramics. These materials are hard and dense and can be manufactured in many shapes and tailored to various applications. The most common type is made of Lead-Zirconate-Titanate (PZT). The piezoelectric effect occurs when a pressure is applied to a material creating an electric charge on the surface of the material and conversely, a change in the dimensions of the material is observed with an applied electric field. Piezopolymers (e.g. Polyvinylidene fluoride, PVDF) are clear plastic films which can also be readily cut and shaped in complex patterns.

Shape memory alloys have the ability to recover a particular shape when activated by an external stimulus. One common type is Nitinol, which is a nickel and titanium alloy that undergoes a reversible phase transformation from austenite to martensite. The shape of the alloy which is to be remembered is formed at the high temperature austenite phase. The alloy can be reshaped below the phase transformation temperature in the martensitic phase. Once the alloy is heated above the transformation temperature, the originally formed shape is remembered, exerting stresses up to 100,000 psi if restrained, or creating strains up to 8% if unrestrained.

Like piezoelectrics, electrostrictive ceramics also change in dimension when an electric field is applied. However, the strain induced is proportional to the square of the electric field, so positive displacements are always realized, i.e. the material cannot contract. Magnetostrictive alloys (e.g. Terfenol-D), expand under the influence of a magnetic field. Electrorheological fluids consist of polarizable, high dielectric constant particles suspended in a dielectric fluid. When exposed to an electric field, the viscosity in these fluids increases.

1.1.2 Actuators

Sensors and actuators are analogous to the nerve and muscle systems, respectively, of a human body that is itself an adaptive system. The signals that are sensed by the sensors and modified by the actuators must be processed in real time under very restrictive conditions. A number of actuator types are available:

Piezoelectric actuators in general, are best suited for high frequency and medium stroke with low to medium power requirements. Piezoelectric crystals tend to be difficult to manufacture and use because of their brittleness. Piezoelectric fibers are an attractive option due to the ease in incorporating them into the manufacturing process, however, they are difficult to produce in long enough lengths to be useful. Piezoelectric ceramics and polymers are both good candidates for adaptive structures. They can be machined to a wide variety of shapes, and have good strength, stiffness, stroke and bandwidth characteristics. However, the application of piezoceramic materials in actuator devices is limited by the material non-linearities and high density. Although the low modulus in piezopolymers often precludes their use as actuators, their high field tolerance and electro-mechanical coupling result in large actuation strains which make them effective actuators in applications where obtaining a good mechanical impedance match is possible.

Electrostrictive devices appear to be especially suited for high frequency and low stroke applications, with lower power requirements. The advantages of constrictive ceramics over piezoelectrics is that they can potentially achieve a larger displacement, hysteresis appears less significant, and since they have a higher density charge, they can produce a greater force when activated.

Furthermore, electrostrictives do not exhibit hysteresis and creep at low frequen-

cies and moderate temperatures, due to the absence of permanent polarization. This gives these materials excellent set point accuracy, which makes these actuators ideal choices for low frequency precision positioning.

Magnetostrictive materials are the magnetic analogy of electrostrictives. Ferromagnetic materials, or magnetostrictors, strain as a result of the interaction between applied magnetic fields and magnetic dipoles in the material. Magnetostrictive materials have a relatively high modulus, they exhibit fast responses and produce large actuation strains. However, the bandwidth of these materials is limited by mechanical resonances, magnetic eddy currents and high energy requirements.

Shape Memory Alloys are ideal actuators for low frequency and high stroke applications, with lower power requirements. Actuator applications are generally in the form of fine wires, which are activated by resistive heating when an electric current is passed through the wire. This heating raises the metal to its austenite temperature inducing it to return to its original shape. The high force and large stroke capability exhibited by these materials make them excellent actuator materials. Fatigue may become a problem, especially if the alloy is deformed to a high strain configuration. Nickel-Titanium alloys (Nitinol) exhibit unique mechanical memory characteristics which make them suitable candidates.

Electro-Rheological (ER) fluids have the property that their viscosity changes drastically upon application of a voltage. This effect has been used to demonstrate an increased damping rate when the ER fluid is activated. ER fluids respond quickly enough to warrant their application in active control, however, they present weight penalties associated with introducing fluid into the structure, and there is uncertainty about whether they can be made to be stable for a long enough period of time. The

most common ER fluids are composed of silicon oil and corn starch.

Mechanical actuators are not considered suitable in adaptive structures applications because they tend to be bulky in size, and embedding the devices in an automated manufacturing process would be difficult.

1.1.3 Sensors

Piezoelectrics sensors use the same type of materials described for use as actuators. The operation of these transducers is essentially a reversible process. They can act as sensors by producing a voltage change in response to deformation. In particular, piezopolymers make excelent sensors due to their low modulus and weight, and they can easily be shaped into many geometries which allows for flexible and unobtrusive use in many sensing applications.

Strain Gages are simple and inexpensive sensors, and represent a mature technology. However, since they are discrete devices, they may be difficult to embed in a composite type structure. This problem can be overcome by producing a thin film with gages printed on it at regular intervals, and subsequently bonding it to the wall of a structure during the manufacturing process.

Fiber Optics make excellent sensors because they are immune to the electromagnetic interference which eliminates costly and heavy shielding that is necessary to support electrical sensors. Additionally, they can be made extremely small and can be embedded into composite materials without structural degradation. The inherent high bandwidth of fiber optic sensors and the data links supporting them enables the potential of systems with a large number of sensors. Finally, because of the high melting point of these fibers and the high inherent strength of glass, they are able

to perform in extremely hostile environments at high temperatures, vibrations and shock loadings.

1.1.4 Control Design and Optimization

There are two levels of control methodology which need to be considered in adaptive structures: local control and global control. In the design of local control, the controller design needs to take into account the large number of actuators and sensors distributed throughout the structure. It may be feasible to use local connections to introduce some level of control or damping into the structure before attempting to close global feedback loops. However, the localized control lacks good performance (Lazarus and Napolitano, 1993). Global control design consists of a centralized controller in which the signals from all the sensors are fed to a centralized processor. The control inputs are then computed and fed back to the distributed actuators. The centralized design has better performance than local control, but is computationally inefficient. A single centralized processor would have to process signals at rates corresponding to the highest mode being controlled, and would have to read all of the inputs and calculate all of the outputs for the entire system. This would impose large computational requirements (typically in the order of [100x100] to [1,000x1,000] computations at speeds of 1,000 Hz) which cannot be achieved even with dedicated real time control computers (capable of computations in the order of [10x10] to [30x30] computations at 1,000 Hz). As a secondary consideration, the centralized scheme requires the transmission of many relatively low level electrical signals, all the way from the sensor to the centralized processing area, thus producing low signal-to-noise ratios.

One approach proposed to address the problems encountered in exclusively local and exclusively gobal control schemes is to use a combination of both, and this is

often referred to as hierarchic or multi-level control architecture (Hall et. al. 1991). In this scheme, there would be two levels of control, a centralized controller for overall performance and distributed processing for local control. Such a structure would be divided into finite control elements with local processors providing local control using measurements made within the element and actuators within the element. An average representation of the shape within each element would then be passed on to the global processor for providing global control. This division of the control function into local and global control has been found to be quite practical, and from an engineering perspective completely reproduces the performance of a truly centralized controller.

Applications of control algorithms such as Linear Quadratic Gaussian/Loop Transfer Recovery (LQG/LTR) and H_∞ algorithms seem to be promising since the structures have normally uncertain and multivariable models. The H_∞ design is attractive because it can cope with a system having many inputs and outputs, and it can guarantee a degree of robustness. Moreover, it is an optimization-based technique which involves the designer in selecting the tuning parameters whilst the complex mathematical algorithms are executed on the computer.

For signal processing in structural control, the interface with sensors and actuators has to be addressed first so that the input and output of a signal processing system can be identified. This interface relates to the sensor type, the number of sensors required and the manner in which they are deployed. From these questions, the type and volume of signals to be processed, the dynamic range of input signals, and the accuracy and speed requirements for processing can be determined. A similar analysis for actuators will provide guidelines for output signal processing. Research in signal processing needs to identify existing signal processing techniques suitable for structural control and formulate signal processing problems that cannot be solved

using existing techniques.

If a structure is to adapt to damage, environmental changes, etc., it must be able to adjust its control scheme in order to track the changes. Optimal control design generally assumes the existence of an accurate plant model. Obtaining this model is the role of system identification techniques when used in adaptive systems. Because of uncertainties such as bonding effects and noise in the process models and measurements, it is very important that appropriate model and parameter identification techniques as well as state estimation techniques be developed.

Finally, for a sensor or actuator to be effective in increasing the damping of a particular mode, it should be positioned as closely as possible to the location of the greatest strain in that mode. This leads to the problem of how to identify the optimal locations of sensors and actuators in order to optimize both the system performance and physical configuration of the system.

For simple systems, engineering judgement may suffice to arrive at an acceptable solution. For more complex systems, such as the ones being considered for space application, the choices are so large that more formal optimization techniques are required. The problem falls into a class of combinatorial optimization for which the solution becomes exceedingly intractable as the problem size increases.

1.2 APPLICATIONS

Numerous applications for adaptive materials have been reported in the literature. For instance, Crawley and de Luis (1991) used piezoceramics, bonded to the surface of cantilever beams, as actuators to excite vibrations and to suppress the vibrations by introducing damping to the system.

Matsubara, Yamamoto and Misumoto (1989) employed piezoelectric dampers to

suppress chatter vibration during a boring process. These piezoelectric dampers were driven so as to generate damping forces corresponding to the vibration velocity of the boring bar. Tzou (1987) demonstrated the control of bending vibration in non-rotating beams by using layered piezoelectric materials.

Palazollo et. al. (1989) and Lin (1990) derived simulation models and demonstrated test results of active vibration control of rotorbearing systems utilizing piezoelectric pushers as actuators.

Adaptive concepts have also been used in vibration suppression of truss structures. Natori et. al. (1989) have proposed a method for vibration control of truss structures using struts as active axial force actuators.

Another aspect in adaptive systems capability is the realization of structures with precise shapes. Miura (1991) proposed a concept where the surface shape of a truss antenna was adjusted by changing the natural length of truss cable members. Belvin, Edighoffer and Herstom (1989) reported the shape adjustment of a 15-meter mesh antenna. The shape adjustment algorithm uses the linearized influence coefficients between adjustment cables and mesh surface. Mitsugi, Yasaka and Miura (1990) studied the shape control concept of the tension truss antenna, where inextensible cables and static determinate conditions are assumed. Tabata et al (1991) have studied shape adjustment for the hybrid tension truss antenna, and it also uses flexible cables for precise shape forming.

Ehlers and Weisshaar (1990) examined the use of embedded active piezoelectric materials to change the aeroelastic stiffness of a lifting surface in order to change flutter characteristics. Scott and Weisshaar (1991) examined the effectiveness of applying piezoelectric actuators to control panel flutter.

The application of adaptive structures technology at the present time is at the

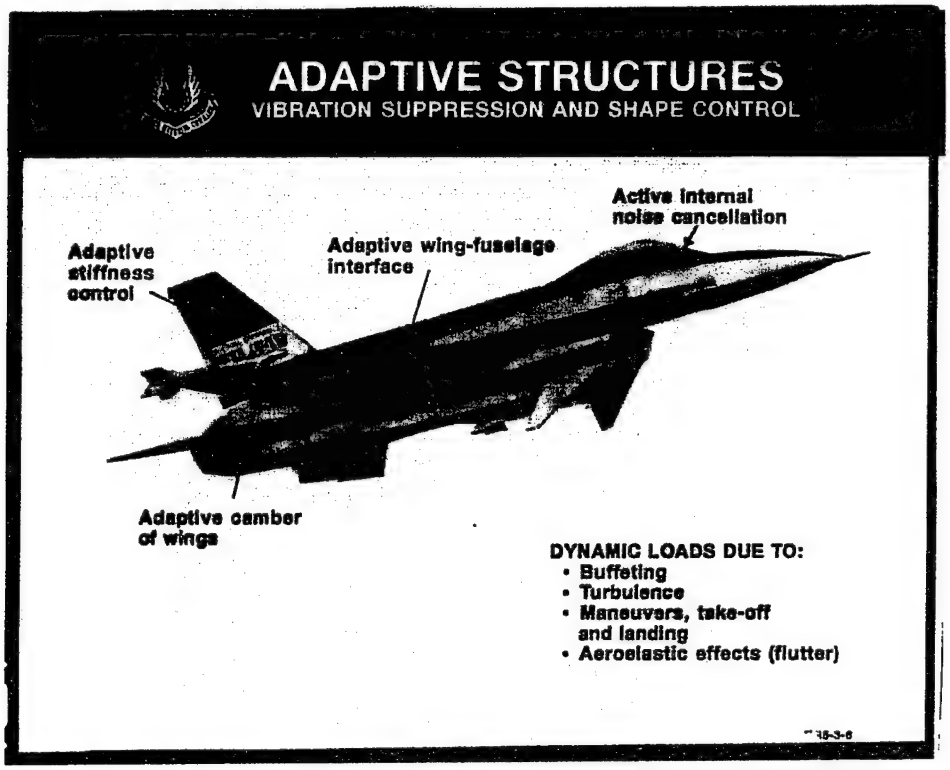

Figure 1.2 Application of adaptive structures technology to aeronautical systems.

research and development stage, as depicted by this brief survey. However, when the technology reaches a mature stage, applications could span the aeronautical, aerospace and ground transportation fields. Aeronautical applications could include attenuation of dynamic loads by means of an active wing fuselage interface or an active wing-engine pylon, flutter vibration suppression by means of adaptive wing camber and active internal cockpit noise cancellation (Figure 1.2). Additional applications have been suggested such as acoustic cavity oscillation, wing/store flutter control, sonic fatigue, gust/load alleviation and airfoil shape control (Lazarus and Napolitano, 1993).

In aerospace systems, such as the proposed Space Station and other large truss

space structures with high performance requirements, vibration control can be attained by using length adjustable active truss members. Another potential application would be in the realization of space structures with precise shapes, such as space antennas of high frequency range and solar collectors.

Ground vehicles are heavily affected by noise and vibration from the motor, road roughness and wind. There are different options for noise and vibration reduction. The most conventional method is to integrate passive damping materials, which unfortunately entails additional weight. More sophisticated is the use of anti-noise loudspeakers in the passenger compartment or in the exhaust system and the use of additional rotating shafts integrated in the motor unit, compensating for the second-order harmonic loads particularly active as a vibration source in engines. Other possible applications include vibration and noise reduction by actively controlled motor suspension systems, attenuation of noise radiation by actively controlling the vibrations of the roof sheets and the splash board, and noise and vibration control by means of an adaptively controlled suspension system.

1.3 PRESENT INVESTIGATION

This brief survey provides a synopsis on current research activities in the field of adaptive materials and structures, and key enabling technologies have been identified to make its implementation a reality. A number of key observations have been made regarding adaptive structures and materials technology: (i) it is a truly multidisciplinary field; (ii) applications are broad based and have been identified; and (iii) considerable benefits are realizable in employment of these concepts.

The present investigation considers the feasibility of applying piezoelectric materials to create restoring forces and bending moments to a flexible structure so that the vibrational response can be tailored to comply with specified performance char-

acteristics.

There are two essential developments in this research. The first is the formulation of a new and considerably simple piezoelectric composite plate finite element based on the Mindlin theory of plates with one electrical degree of freedom per piezoelectric layer. By modelling the plate and the sensor/actuator system with quadrilateral shell elements, the locking problems associated with the solid element are eliminated and the problem size is considerably reduced.

Second, the effectiveness of using an adaptive composite panel to control flutter is examined. First order piston theory is used to model the supersonic flow. The piezoelectric actuators are used passively to induce inplane forces to alter the panel stiffness characteristics, thus increasing the flutter boundary envelope.

CHAPTER
TWO

ELECTROMECHANICAL FINITE ELEMENT COMPOSITE PLATE MODEL

Numerous analytical and finite element modelling techniques have been considered to incorporate the piezoelectric behaviour into beam, plate and shell type structures. For example, Crawley and De Luis (1985) developed a Rayleigh-Ritz analytical model for distributed segmented piezoelectric actuators bonded to an elastic structure.

Lee (1990) and Wang and Rogers (1991) applied classical laminated theory to a composite plate with induced strain actuators, either bonded to the surface or embedded within the laminate. In their study, the thickness and size of the actuator patches were assumed to be relatively smaller than those of each lamina, so the actuator patches were neglected for calculating the global properties of the laminate.

Tzou and Gadre (1989) derived a finite element formulation for multi-layered shells coupled with piezoelectric shell actuators. Ha, Keilers and Chang (1992) also developed a finite element formulation for modelling the response of laminated composites containing piezoceramic materials. Herein, the plate and the thin piezoelectric actuators and sensors were modelled using the isoparametric hexahedron solid element. However, the use of solid elements makes the problem size large and unsuitable for control applications. Therefore, techniques such as Guyan reduction are used to keep the problem size tractable. Other problems associated with the isoparametric solid element in thin plate bending analysis are the excessive shear strain energies

and the higher stiffness coefficients in the thickness direction.

Here, a finite element plate bending formulation with an arbitrary number of piezoelectric layers embedded in a composite plate type structure is presented. The direct and converse piezoelectric phenomena, involving the interaction between the mechanical and electrical behaviour of the material is modelled by linear constitutive equations involving two mechanical variables (stress and strain) and two electrical variables (electric field and displacement).

2.1 FINITE ELEMENT FORMULATION

The finite element model selected in this study is a four-node, bilinear displacement element based upon the Mindlin theory of plates (Mindlin, 1951). Such elements exhibit good accuracy for both thick and thin plates when reduced (one-point) numerical integration is used to evaluate the element matrices. However, the resulting element is rank deficient, and must be stabilized to achieve reliable behaviour. Methods for achieving full rank of the stiffness and for stabilizing element behaviour in static analysis and in explicit dynamic calculations exist and are quite effective (Brockman, 1989).

2.1.1 Mindlin Plate Theory

Plate theory is derived from the three-dimensional theory of elasticity by the introduction of simplifying approximations. There are three mathematical models for thin plate motion: the fourth-order Kirchhoff model, the sixth-order Mindlin model and the nonlinear von Karman model. The Kirchhoff and the Mindlin models are "small-displacement" linear models. The Mindlin model incorporates transverse shear effects while the Kirchhoff model does not. The sixth-order Mindlin model is a hyperbolic system of three coupled second-order partial differential equations in two

independent variables. The unknowns are the transverse component of displacement w and the rotations θ_x and θ_y, which are measures of the transverse shear effects. The three equations are coupled through the shear modulus constant.

The von Karman model is a large deflection plate model represented by a coupled pair of fourth order, nonlinear partial differential equations for the vertical displacement w. The coupling takes place through quadratic nonlinearities in the second-order spatial derivative of w.

From a finite element discretization point of view, Kirchhoff elements generally do not use second derivatives of the field variable as nodal degrees of freedom thus violating C^1 continuity either because slope continuity is not enforced on exterior edges or because the second derivatives of the field are discontinuous at interior points. In Mindlin plate theory, since the transverse shear strain is allowed a nonzero value, the rotations of the normal θ_x and θ_y become independent variables, and the C^1 continuity requirement for w tranlates into C^0 continuity requirements for w, θ_x and θ_y.

The quadrilateral Mindlin plate finite element with bilinear displacement and rotation fields, based on single-point quadrature, was introduced by Hughes, Cohen, and Haroun (1978). Brockman (1989) has developed and implemented this finite element into PROTEC, and the following brief literature review is an excerpt from his report. The attractiveness of such an element stems from its simplicity, computational efficiency, and high accuracy since the single quadrature point is an optimal sampling point (Zienkiewicz, O.C., 1977). However, the element is rank deficient, since bilinear contributions to the displacement field are not captured by the single point integration. Therefore, the assembled stiffness may exhibit singularities when properly constrained, or lead to the prediction of spurious oscillatory displacements

with little or no strain energy associated.

Subsequent development of the bilinear Mindlin plate element focused largely on the stabilization of these spurious modes of behaviour. In the context of explicit dynamic computations, the concept of hourglass stabilization, as discussed by Kosloff and Frazier (1978) and further developed by Flanagan and Belytschko (1981) and Belytschko, Lin and Tsai (1984) is an effective means of controlling this behaviour. However, the explicit solution provides an opportunity for individual elements to "react" to unstable oscillatory motions, while a static or implicit dynamic solution does not.

MacNeal (1978), and Hughes and Tezduyar (1981) have proposed schemes for stabilizing the bilinear element by redefining the interpolation of the transverse shear strain field. However, these techniques require a four-point quadrature, and the simplicity of the basic element is lost. Taylor (1979) and Belytschko et al. (1981, 1983) have pursued the idea of hourglass mode stabilization for static analysis, and present several correction methods which work well while perserving the advantages of the one-point integration scheme. Park, Stanley and Flaggs (1985) have presented related methods of stabilization, obtained as a by-product of studies on element behaviour with increasing mesh refinement.

2.1.2 Electromechanical Plate Finite Element

The kinematic assumptions of Mindlin plate theory (Mindlin, 1951) relate the displacements (U, V, W) at a generic point in a flat plate to displacements (u, v, w) and rotations (θ_x, θ_y) of the midsurface by:

$$U(x,y,z) = u(x,y) + z\theta_y(x,y);$$

$$V(x,y,z) = v(x,y) - z\theta_x(x,y);$$

$$W(x, y, z) = w(x, y),$$

where z is the direction normal to the midsurface. The state of deformation is described by eight generalized strains

$$\bar{\epsilon}^T = \left[\epsilon_x, \epsilon_y, \gamma_{xy}, \kappa_x, \kappa_y, \kappa_{xy}, \gamma_{xz}, \gamma_{yz}\right]$$

and the stress state by the corresponding generalized forces,

$$\bar{\sigma}^T = \left[N_x, N_y, N_{xy}, M_x, M_y, M_{xy}, Q_{xz}, Q_{yz}\right].$$

Now, consider a laminated composite plate containing distributed piezoelectric layers that can be either bonded to the surface or embedded within the structure as shown in Figure 2.1.

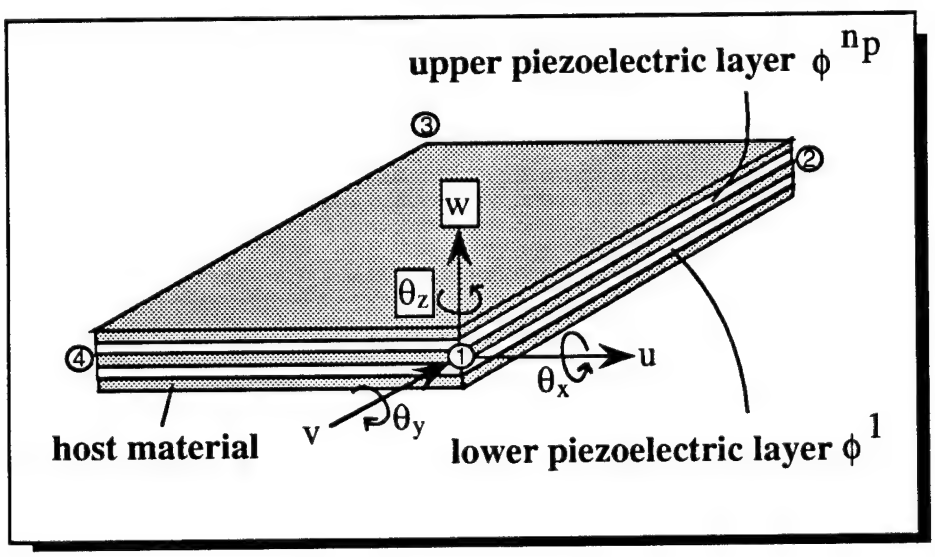

Figure 2.1 Finite element composite plate element showing the displacement degrees of freedom for the mechanical elastic properties and the electrical degrees of freedom for the piezoelectric behaviour.

To derive the equations of motion for the laminated composite plate, with piezoelectrically coupled electromechanical properties, we use the generalized form of Hamilton's principle

$$\delta \int_{t_1}^{t_2} \left[T - \Pi + W_e\right] dt = 0 \tag{1.1}$$

where T is the kinetic energy, Π is the potential energy, and W_e is the work done by the electrical field. The kinetic and potential energies can be written in the form

$$T = \int_V \frac{1}{2}\rho \dot{\bar{u}}^T \dot{\bar{u}} dV; \qquad \Pi = \int_V \frac{1}{2} \bar{S}^{c^T} \bar{T}^c dV$$

where $\bar{S}^c$ and $\bar{T}^c$ are the generalized elastic strain and stress vectors. The work done by the electrical forces can be written as

$$W_e = \int_{V_p} \frac{1}{2} \bar{S}^{e^T} \bar{T}^e dV_p$$

where $\bar{S}^e$ is a vector of electrical fields (potential/length) in the piezoelectric material, and $\bar{T}^e$ is a vector of electrical displacements (charge/area).

2.1.3 Constitutive Relations

For piezoelectrics, the properties are defined relative to the local poling direction. Available piezoelectric materials have the direction of poling associated with the transverse direction (Figure 2.2), and the material is approximately isotropic in the other two directions. In matrix form the equations governing these material properties can be written as

$$\bar{T}^e = \mathbf{e}^{\mathbf{T}}\, \bar{S}^c + \epsilon\, \bar{S}^e$$

$$\bar{T}^c = \mathbf{c}\, \bar{S}^c - \mathbf{e}\, \bar{S}^e$$

where $\bar{T}^e$ is the electric displacement vector; $\mathbf{e}$ is the dielectric permittivity matrix; $\bar{S}^c$ is the elastic strain vector; ϵ is the dielectric matrix at constant mechanical strain;

$\overline{S}^e$ is the electric field vector; $\overline{T}^c$ is the elastic stress vector and $\mathbf{c}$ is the matrix of elastic coefficients at constant electric field strength.

2.1.4 Strain-Displacement Relations

The state of deformation is described by eight generalized strains and one electrical field parameter per lamina. Thus, the augmented generalized strain vector takes the form

$$\begin{aligned}\bar{S} &= \{\bar{S}^m \quad \bar{S}^b \quad \bar{S}^{ts} \quad \bar{S}^e\} \\ &= \{S_x^m \quad S_y^m \quad S_{xy}^m \quad S_x^b \quad S_y^b \quad S_{xy}^b \quad S_{xz}^{ts} \quad S_{yz}^{ts} \quad -E_1 \quad \ldots -E_{n_p}\}\end{aligned}$$

where n_p is the number of piezoelectric layers in the element. For the bilinear finite element with four nodal points, we use the shape functions:

$$\mathbf{N} = \frac{1}{4}(\bar{C} + \bar{\xi}\xi + \bar{\eta}\eta + \bar{H}\xi\eta)$$

in which

$$\begin{aligned}\bar{C}^T &= [\ 1,\ \ 1,\ \ 1,\ \ 1]; \\ \bar{\xi}^T &= [-1,\ \ 1,\ \ 1, -1]; \\ \bar{\eta}^T &= [-1, -1,\ \ 1,\ \ 1]; \\ \bar{H}^T &= [\ 1, -1,\ \ 1, -1].\end{aligned}$$

There are six displacement degrees of freedom at each node for the elastic behaviour, and there is one potential degree of freedom per layer for the piezoelectric effect. Thus

$$\begin{aligned}\bar{q}_i^c &= \{u \quad v \quad w \quad \theta_x \quad \theta_y \quad \theta_z\}_i; \qquad i = 1, \ldots, 4 \\ \bar{q}^e &= \{\phi_1 \quad \ldots \phi_{n_p}\}\end{aligned}$$

The strain-displacement relations for the bilinear element are based on first order

shear deformation theory and the electric field-potential relations $\bar{S}^e = -\nabla.\phi$. The potential degrees of freedom are constant along the face of the piezoelectric layer and they are assumed to vary linearly through the thickness. Thus the matrix relating the generalized strains to the nodal displacements and electric potentials can be written as follows:

$$\bar{S} = \begin{Bmatrix} \bar{S}^c \\ \bar{S}^e \end{Bmatrix} = \begin{bmatrix} \mathbf{b}^c & 0 \\ 0 & \mathbf{b}^e \end{bmatrix} \begin{Bmatrix} \bar{q}^c \\ \bar{q}^e \end{Bmatrix}$$

where

$$\mathbf{b}_i^c = \begin{bmatrix} \frac{\partial N_i}{\partial x} & 0 & 0 & 0 & 0 & 0 \\ 0 & \frac{\partial N_i}{\partial y} & 0 & 0 & 0 & 0 \\ \frac{\partial N_i}{\partial y} & \frac{\partial N_i}{\partial y} & 0 & 0 & 0 & 0 \\ 0 & 0 & 0 & 0 & z\frac{\partial N_i}{\partial x} & 0 \\ 0 & 0 & 0 & -z\frac{\partial N_i}{\partial y} & 0 & 0 \\ 0 & 0 & 0 & -z\frac{\partial N_i}{\partial x} & z\frac{\partial N_i}{\partial y} & 0 \\ 0 & 0 & \frac{\partial N_i}{\partial x} & 0 & N_i & 0 \\ 0 & 0 & \frac{\partial N_i}{\partial y} & -N_i & 0 & 0 \end{bmatrix}$$

$$\mathbf{b}^e = \begin{bmatrix} \frac{1}{t_1} & \cdots & 0 \\ \vdots & \ddots & \vdots \\ 0 & \cdots & \frac{1}{t_{n_p}} \end{bmatrix}$$

2.1.5 Stress-Strain Relations

The composite laminate plate is persumed to consist of perfectly bonded laminae. Moreover, the bonds are presumed to be infinitesimally thin as well as non-shear-deformable. Thus, following classical lamination theory (Jones, 1975), the state of stress in the element is given by

$$\begin{aligned} \bar{T} &= \{\bar{T}^m \quad \bar{T}^b \quad \bar{T}^{ts} \quad \bar{T}^e\} \\ &= \{T_x^m \quad T_y^m \quad T_{xy}^m \quad T_x^b \quad T_y^b \quad T_{xy}^b \quad T_{xz}^{ts} \quad T_{yz}^{ts} \quad D_1 \quad \ldots \quad D_{n_p}\} \end{aligned}$$

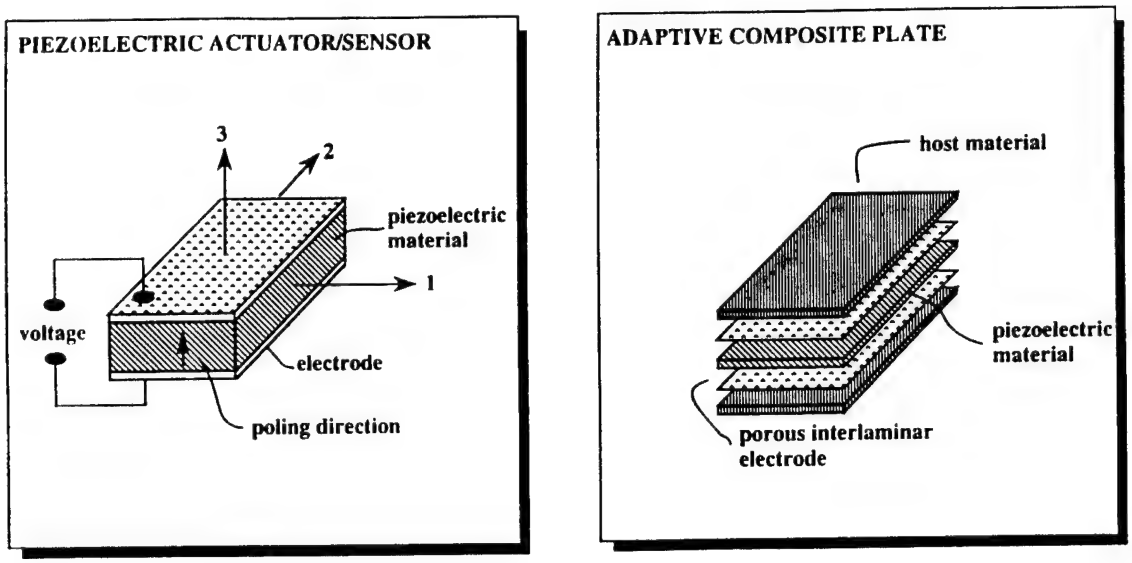

Figure 2.2 Piezoelectric patch showing direction of polarization and electrode layout.

and the stress-strain relationship takes the form

$$\bar{T} = \begin{Bmatrix} \bar{T}^c \\ \bar{T}^e \end{Bmatrix} = \begin{bmatrix} \mathbf{c} & \mathbf{c} & \mathbf{0} & \mathbf{e} \\ \mathbf{c} & \mathbf{c} & \mathbf{0} & \mathbf{e} \\ \mathbf{0} & \mathbf{0} & \mathbf{g} & \mathbf{0} \\ \mathbf{e}^T & \mathbf{e}^T & \mathbf{0} & \epsilon \end{bmatrix} \begin{Bmatrix} \bar{S}^m \\ \bar{S}^b \\ \bar{S}^{ts} \\ \bar{S}^e \end{Bmatrix}$$

where $\mathbf{c}$ is the transformed moduli matrix for each lamina including the piezoelectric layers. The transverse shear stiffness matrix $\mathbf{g}$ is defined in terms of the transverse strain energy through the thickness. Substituting for the generalized stress and strain expressions into Equation (1.1), we obtain the mass, elastic stiffness and piezoelectric stiffness matrices:

$$\mathbf{M}^{\mathbf{j}}{}_{cc} = \int_{V_j} \rho \mathbf{N}^T \mathbf{N} dV_j, \qquad j = 1, \ldots, n_{el};$$

$$\mathbf{K}^{\mathbf{j}}{}_{cc} = \int_{V_j} \mathbf{b}^{\mathbf{c}T} \mathbf{c} \mathbf{b}^{\mathbf{c}} dV_j, \qquad j = 1, \ldots, n_{el};$$

$$\mathbf{K}^{\mathbf{j}}{}_{ce} = \int_{V_j} \mathbf{b}^{\mathbf{c}T} \mathbf{e} \mathbf{b}^{\mathbf{e}} dV_j, \qquad j = 1, \ldots, n_{el};$$

$$\mathbf{K}^{\mathbf{j}}{}_{ee} = \int_{V_j} \mathbf{b}^{\mathbf{e}T} \mathbf{e} \mathbf{b}^{\mathbf{e}} dV_j, \qquad j = 1, \ldots, n_{el}.$$

In the stress-strain relationships for the in-surface strains and curvatures, plane stress assumptions are used. The transverse shear quantities are related by $Q_{\alpha z} = kGt\gamma_{\alpha z}$, in which k is a shear correction factor (Whitney, 1973); here we employ the value $k = \frac{5}{6}$.

2.2 EQUATIONS OF MOTION

For the entire structure, using the standard assembly technique for the finite element method and applying the appropriate boundary conditions, we obtain the complete equations of motion for a piezoelectrically coupled electromechanical composite panel

$$\overbrace{\begin{bmatrix} \mathbf{M}_{cc} & \mathbf{0} \\ \mathbf{0} & \mathbf{0} \end{bmatrix}}^{Inertia} \begin{Bmatrix} \ddot{\bar{U}}^c \\ \ddot{\bar{U}}^e \end{Bmatrix} + \overbrace{\begin{bmatrix} \mathbf{K}_{cc} & \mathbf{0} \\ \mathbf{0} & \mathbf{0} \end{bmatrix}}^{Elastic\,Stiffness} \begin{Bmatrix} \bar{U}^c \\ \bar{U}^e \end{Bmatrix} + \overbrace{\begin{bmatrix} \mathbf{0} & \mathbf{K}_{ce} \\ \mathbf{K}_{ec} & \mathbf{K}_{ee} \end{bmatrix}}^{Piezo\,Stiffness} \begin{Bmatrix} \bar{U}^c \\ \bar{U}^e \end{Bmatrix} = 0 \quad (1.2)$$

where $\mathbf{M}_{cc}$ is the mass matrix of the structure with the piezoelectric layers, $\mathbf{K}_{cc}$ is the mechanical stiffness matrix, $\mathbf{K}_{ee}$ is the piezoelectric stiffness matrix, and $\mathbf{K}_{ec}$ is the coupled electrical/mechanical stiffness matrix.

2.3 SIMULATION RESULTS

To demonstrate the perfomance of the finite element formulation developed here, several comparison studies are presented here. The numerical results were compared to experiments and simulations documented in the literature.

2.3.1 Static Actuation and Sensing

The first validation test case was based on an experiment conducted by Tzou and Tseng (1990). The experimental apparatus consists of a cantilevered piezoelectric

bimorph beam with two PVDF layers bonded together and polarized in opposite directions (Figure 2.3a). The model was divided into five equal elements, each with two piezoelectric layers bonded together. This produced a finite element model with 53 total degrees of freedom (Figure 2.3b).

First, the actuation mechanism, derived from Equation (1.2), and expressed as

$$\bar{U}^c = -\mathbf{K}_{cc}^{-1}\mathbf{K}_{ce}\bar{U}^e$$

is investigated. The top and bottom surface of the beam were subjected to an electric potential across the thickness of the beam and the resulting displacements were determined. A unit voltage (± 5 V for the top and bottom layers, respectively) produces a tip deflection of $3.45 \times 10^{-7} m$ as shown by the results tabulated in Figure 2.3(c). It is observed that there is no difference between the results evaluated by the composite finite element model and the theoretical results. The slightly lower tip deflection observed in the experiment could be caused by non-perfect bonding, voltage leakage, energy dissipation, etc. The total number of degrees of freedom used in this analysis (63 = 53 structural + 10 electrical) is considerably lower than the model studied by Tzou and Tseng (144 = 108 structural + 36 electrical), resulting in a lower computational memory requirement.

The bimorph beam is also studied for sensing voltage distribution for a prescribed static deflection. This is the sensing mechanism, governed by

$$\bar{U}^e = -\mathbf{K}_{ee}^{-1}\mathbf{K}_{ec}\bar{U}^c.$$

When external tip loads are applied to produce a given deflection pattern, the electrical degrees of freedom output a sensing voltage. The results in Figure 2.3(d) show that a voltage of 290 V is sensed for an imposed tip deflection of 1 cm. The results are in good agreement with the solid finite element solution. However, since the finite

plate element used in this study guarantees the continuity of strains due to bending, i.e. rotation at the nodes, the accuracy of sensing may be higher than the brick element that guarantees only displacement continuity at the nodes. Furthermore, it can be observed that while the results for Tzou and Tseng (1990) are given in terms of nodal voltages, the present theory produces elemental voltages, constant over each piezoelectric layer.

The second case was based on the experiments conducted by Crawley and Lazarus (1991). The experimental apparatus consists of a cantilevered laminated composite graphite/epoxy plate with distributed G-1195 piezoceramic (PZT) actuators bonded to the top and bottom surfaces (Figure 2.4a). The finite element model consists of 160 elements with a total of 880 degrees of freedom (Figure 2.4b). During actuation, a constant voltage with an opposite sign was applied to the actuators on each side of the plate. The deflections of the center line and both edges were measured by proximity sensors. Figure 2.4(c) shows the comparison of the deflection due to longitudinal bending for a $[0/\pm 45]_s$ layup between the present plate formulation, the solid brick finite element model and the experimental results. All the solutions are in close agreement, with lower deflection observed for the solid element formulation due to shear locking effects associated with solid finite element models. The discrepancy observed in the experimental results may be attributed to shear losses in the bonding layers. Figure 2.4(d) shows the deformed configuration of the cantilevered plate resulting from the static actuation.

For sensing, the comparisons are conducted against the numerical simulations performed by Ha, Keilers and Chang (1992). During this simulation, the center row of piezoceramics were considered sensors while the outer two rows were used as actuators. A constant voltage of 100 V was applied to one row of actuators with a

positive sign on the top surface and a negative sign on the bottom surface. The same voltage was applied to the other row but in this instance the polarity was reversed, thus inducing a twisting motion to the plate. Furthermore, a constant mechanical load of 0.2 N was applied at the tip of the plate. Thus, the output sensor voltages were numerically determined for the combination of electrical and mechanical loads. Figure 2.4(e) shows good agreement between the solid brick finite element model and the composite plate model formulations and Figure 2.4(f) shows the sensed voltages along the central tier of piezoelectric patches.

Finally, consider the same cantilever plate with only two pairs of piezoelectric patches located near the clamped boundary. It was of interest to determine the amount of voltage required by the piezoelectrics to maintain a zero tip deflection of the plate, when subjected to a concentrated load at the tip. The voltage required to preserve the zero tip deflection as a function of the applied mechanical loading is presented in Figure 2.5(a). It is observed that a linear relationship between the voltage and the applied load exists. Figure 2.5(b) shows the deformation of the plate under both the mechanical loading and the calculated electrical loading, with the piezoelectric layers in actuation.

2.3.2 Eigenvalue Solution

The experimental apparatus used in this experiment consists of an aluminum cantilever beam with six pairs of lead zirconate titanate (PZT) tiles attached to the locations shown in Figure 2.6(a). This experiment was set up by Hollkamp (1994) at the Wright Laboratory. A measurement/excitation spectrum analyzer is connected to the structure to carry out control studies in the frequency domain. The natural frequencies of the first three bending modes have been estimated using experimental data. The natural frequencies are $f_1 = 9.2$, $f_2 = 57.5$ and $f_3 = 160.5$ Hz. The

finite element model used to simulate this structure is comprised of 26 elements, 195 structural degrees of freedom, and 24 electrical degrees of freedom (Figure 2.6b). The frequencies estimated by the finite element model are $f_1 = 9.1$, $f_2 = 58.2$ and $f_3 = 168.3$ Hz.

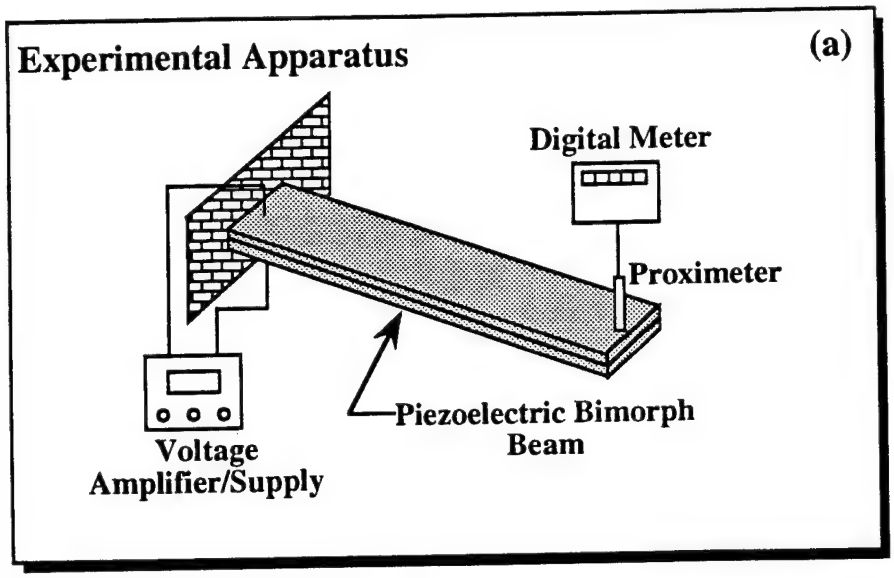

Figure 2.3 (a) Test study comparison between the present formulation and Tzou and Tseng (1990) showing the experimental apparatus for the piezoelectric bimorph plate.

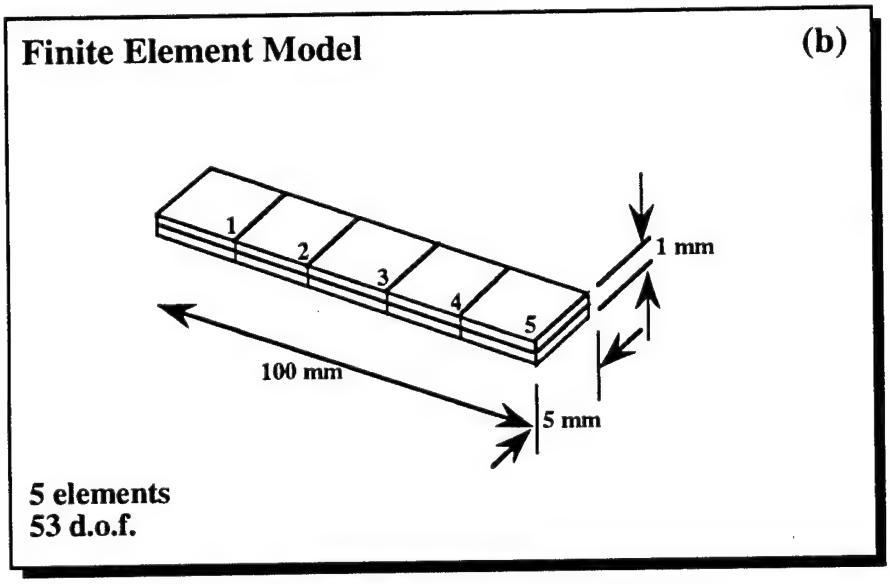

Figure 2.3 (b) Test study comparison between the present formulation and Tzou and Tseng (1990) showing the finite element model with 53 degrees of freedom.

Actuation Mechanism (c)

$x10^{-7}$ m

Position	1	2	3	4	5
Theory	0.14	0.55	1.24	2.21	3.45
Beam FE[6]	0.12	0.51	1.16	2.10	3.30
Present	0.14	0.55	1.24	2.21	3.45
EXP[6]	-	-	-	-	3.15

Figure 2.3 (c) Test study comparison between the present formulation and Tzou and Tseng (1990) showing the comparison of results for the static actuation mechanism.

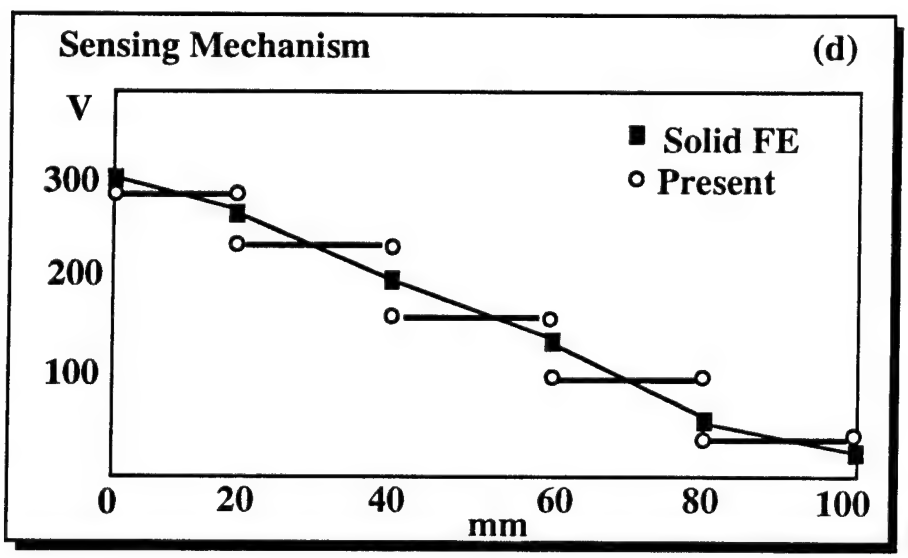

Figure 2.3 (d) Test study comparison between the present formulation and Tzou and Tseng (1990) showing the static sensing mechanism.

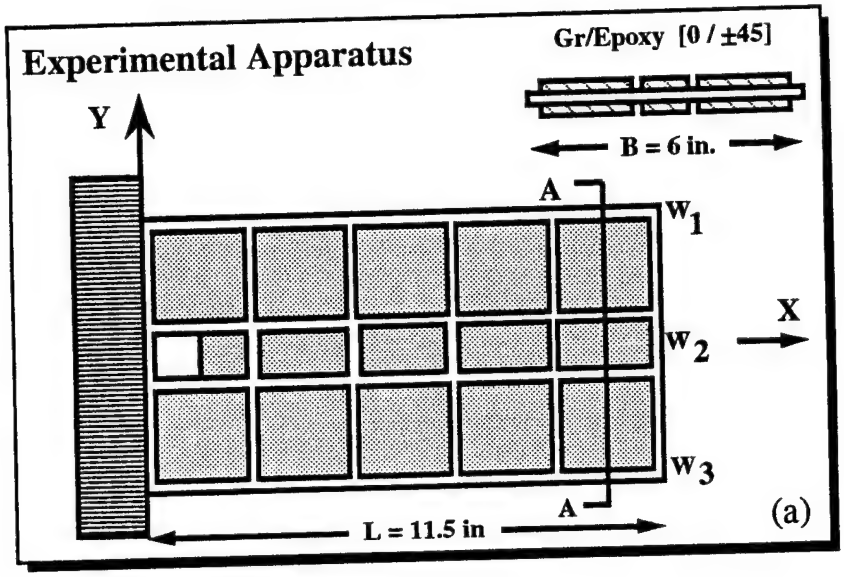

Figure 2.4 (a) The experimental apparatus showing the Gr/Epoxy [0/±45] cantilevered plate studied by Crawley and Lazarus (1991).

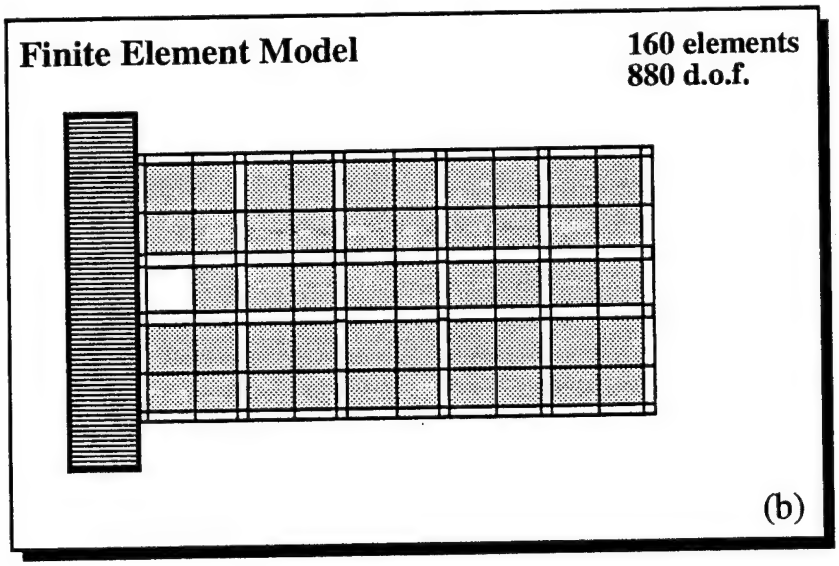

Figure 2.4 (b) The finite element model with 880 degrees of freedom developed here to compare the results with the model reported by Crawley and Lazarus (1991) .

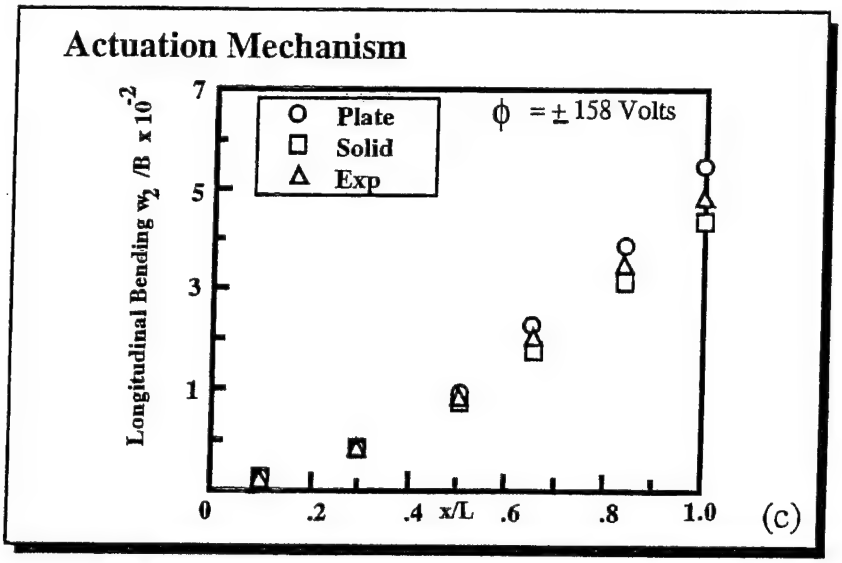

Figure 2.4 (c) Comparison between the present formulation results and Crawley and Lazarus (1991) showing the results for the static actuation mechanism.

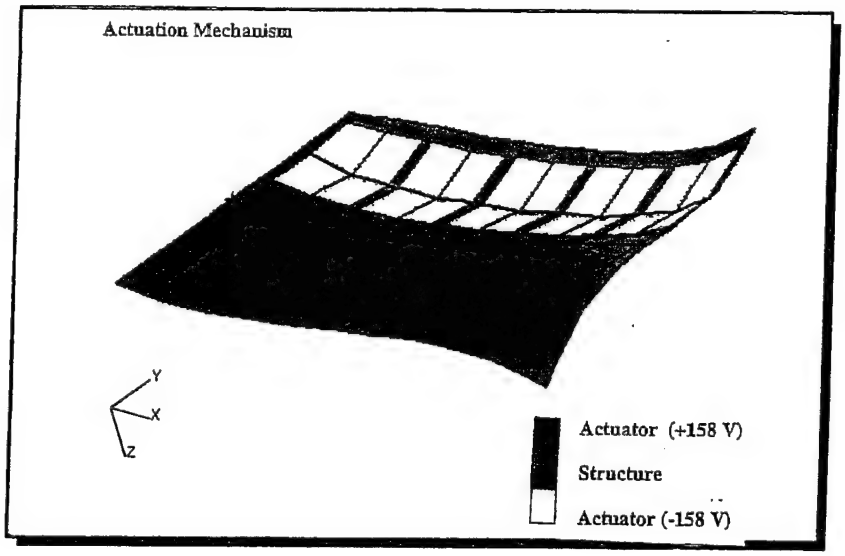

Figure 2.4 (d) The deformed configuration of the cantilevered plate resulting from the static actuation for an applied voltage of $\pm 158V$.

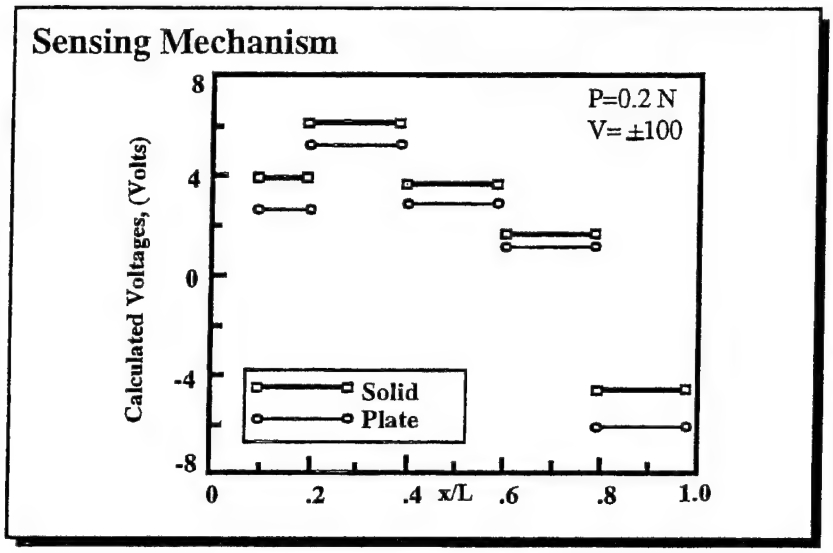

Figure 2.4 (e) Comparison of the sensing voltages along the central tier of piezoelectric elements due to voltage of $\pm 100V$ applied on the outer tiers of piezoelectrics.

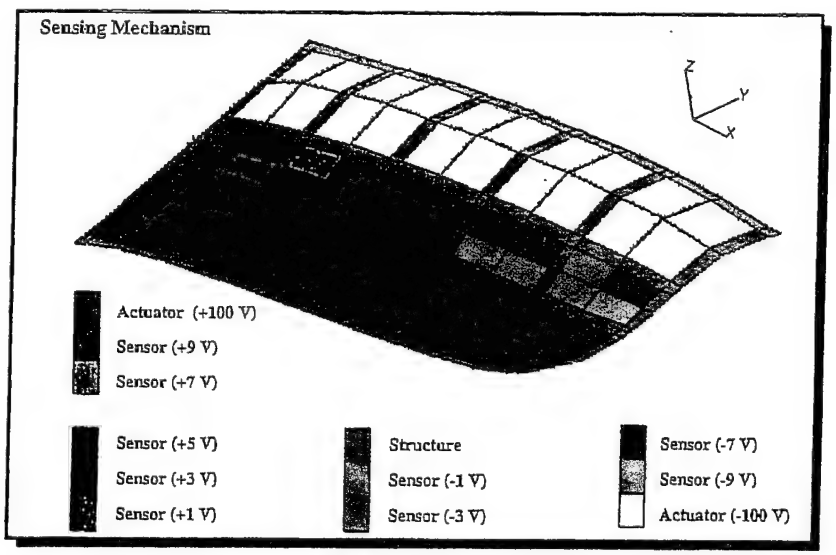

Figure 2.4 (f) The deformed configuration showing the sensed voltages along the central tier of piezoelectrics.

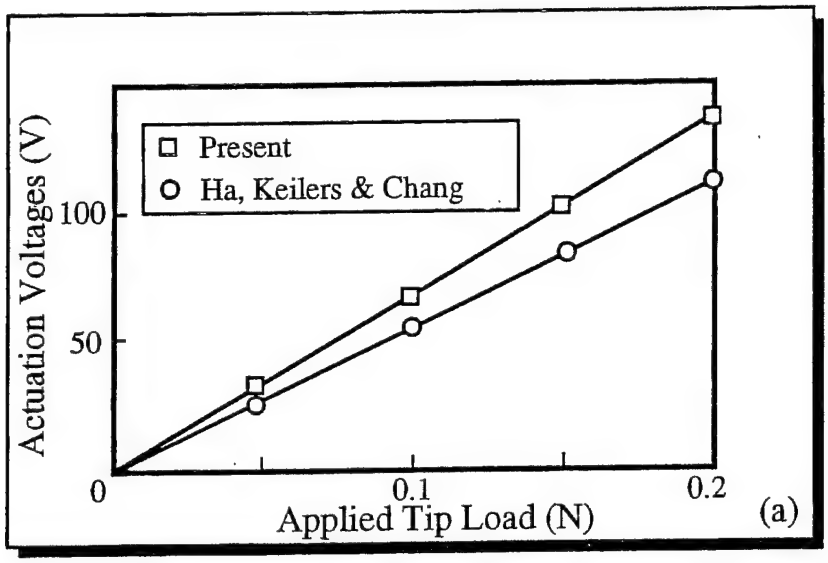

Figure 2.5 (a) Comparison between the present formulation and Ha, Keilers and Chang (1992) showing the relationship between the required actuation voltages and the various tip loading conditions.

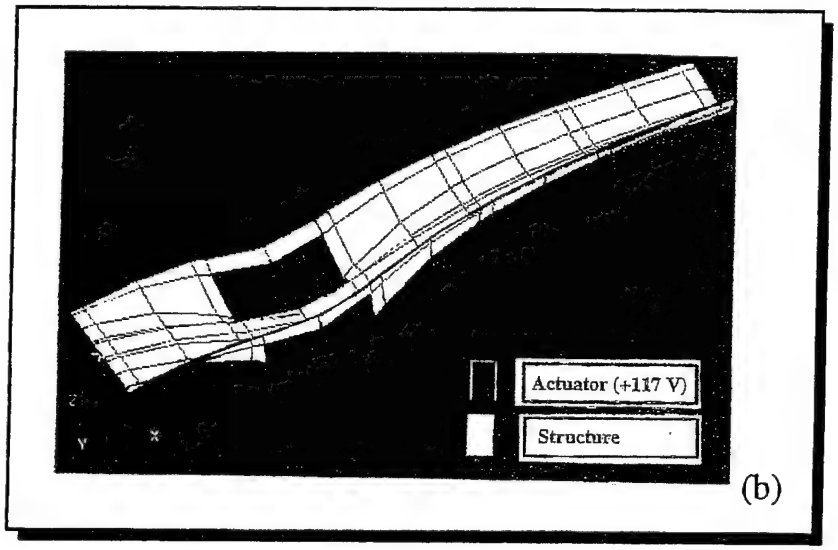

Figure 2.5 (b) The deformed configuration of the cantilevered plate under the action of the mechanical tip load and electric actuation.

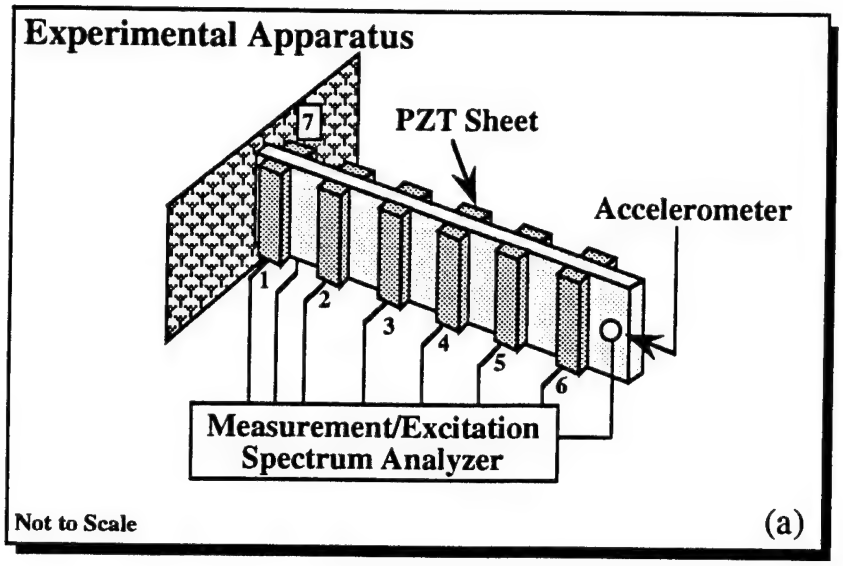

Figure 2.6 (a) Eigenvalue solution comparison between the present formulation and Hollkamp (1994) showing the experimental apparatus for the aluminum cantilever beam with 6 pairs of PZT tiles.

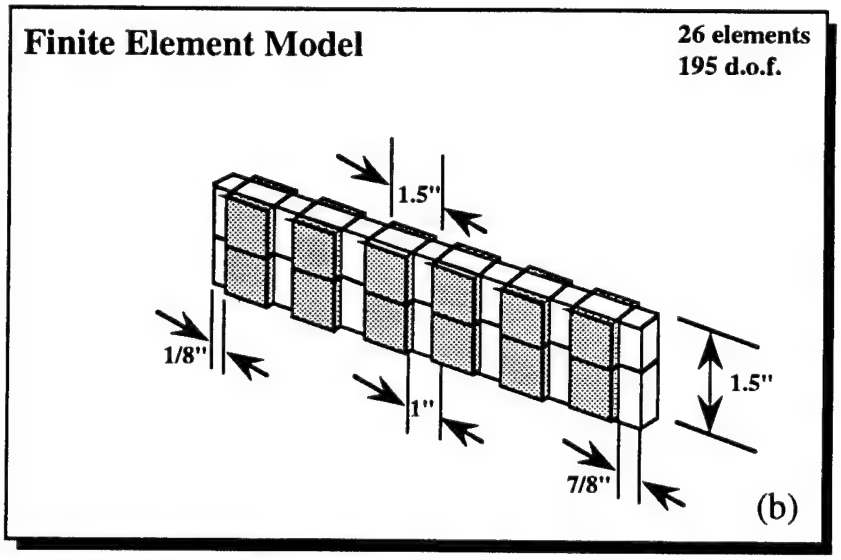

Figure 2.6 (b) Natural frequencies comparison between the present formulation and Hollkamp (1994) showing the finite element model with 195 degrees of freedom.

2.4 COMMERCIAL FEM CODES

A few finite element commercial codes have incorporated piezoelectric modelling features and four codes are analyzed here and their capabilities are reported.

2.4.1 ANSYS - Swanson Analysis Systems, Inc.

In ANSYS, the piezoelectric analysis is a feature of the coupled-field analysis capability. The following finite elements are available in ANSYS (Swanson Analysis, 1986) to perform a coupled-field piezoelectric analysis: PLANE13 (the 2-D coupled-field solid), SOLID5 (the 3-D coupled field solid), and SOLID98 (the 3-D coupled-field tetrahedron). The analysis may be static, modal, harmonic, or transient. Other types of coupled-field analysis are available using these elements such as thermal-stress analysis, thermal-electric analysis, electro-magnetic analysis, magnetic-structural analysis and magnetic-thermal analysis.

To perform a piezoelectric analysis, the dielectric constant $[\epsilon^E]$ can be input by using the MP command. Only the diagonal components of the dielectric matrix can be input (PERX,PERY, PERZ). The TB,PIEZ and TBDATA commands are used to define the $[e]$ matrix. The elastic coefficient matrix $[c]$ can be input by either using the TB, ANEL and TBDATA commands or by using the MP,EX and MP,NUXY commands. A typical input data card deck would have the form shown in Table 2-1.

2.4.2 ABAQUS - Hibbit, Karlsson & Sorensen, Inc.

In ABAQUS (Hibbit, Karlsson and Sorensen Inc., 1990), a fully coupled piezoelectric analysis may be performed for continuum problems in one, two and three dimensions. The elements that provide this capability are the piezoelectric plane strain elements (CPE3E, CPE4E, CPE6E, CPE8E, CPE8RE), the piezoelectric plane stress elements (CPS3E, CPS4E, CPS6E, CPS8E, CPS8RE), all with active degrees of free-

Table 2-1 Input data card deck for ANSYS showing the necessary commands to perform a piezoelectric analysis.

ANSYS INPUT DATA

```
/PREP7
ET,1,SOLID5
MP,EX,... (Young's Modulus)
MP,NUXY,... (Poisson's Ratio)
MP,PERX,... (Dielectric Matrix [ε])
TB,PIEZ,1 (Piezoelectric Matrix [e])
TBDATA,...
FINISH
/SOLUTION
ANTYPE,STATIC
D,ALL,UX,0,,,,UY,UZ (Constraints)
D,ALL,VOLT,...
SAVE
SOLVE (Solution Phase)
FINISH
```

dom 1,2 and 9 (Ux, Uy and ϕ), and the piezoelectric solid elements (C3D4E, C3D6E, C3D8E, C3D10E, C3D15E, C3D20E and C3D20RE), with active degrees of freedom 1,2,3 and 9 (Ux, Uy, Uz and ϕ). The materials electrical and electro-mechanical coupling behaviour are defined by its dielectric property and its piezoelectric stress property. These properties may be entered using the *PIEZOELECTRIC and *DIELECTRIC cards. A typical ABAQUS data input deck would have the form shown in Table 2-2.

2.4.3 NASTRAN(CSA) - CSAR Corporation

The piezoelectric theory in CSA-NASTRAN (CSAR Corporation, 1980) has been incorporated into the finite element formulations of the TRAPAX and TRIAAX elements. These elements, trapezoidal and triangular in cross-section respectively, are solid, axisymmetric rings whose degrees of freedom are expanded into Fourier se-

Table 2-2 Input data card deck for ABAQUS showing the necessary commands to perform a piezoelectric analysis.

ABAQUS INPUT DATA

```
*NODE, NSET=TOP (Input Nodal Coord.)
*ELEMENT, TYPE=C3D20E,
          ELSET=PID1
*SOLID SECTION,ELSET=PID1,
           MATERIAL=PVDF
*MATERIAL, NAME=PVDF
*ELASTIC, TYPE=ISO
*PIEZOELECTRIC, TYPE=S
*DIELECTRIC, TYPE=ISO
*STEP, PERTURBATION
*STATIC (Solution Phase)
*BOUNDARY (Constraints)
```

ries, thus allowing non-axisymmetric loads. The degrees of freedom per node are the radial, tangential and axial displacements and the electric potential.

Piezoelectric modelling requires the specification of a parameter on the NASTRAN card as well as the use of up to four bulk data cards. The NASTRAN card allows the user to override various NASTRAN system parameters by defining specific words in the /SYSTEM/ COMMON block. The 78th word of /SYSTEM/, that is, SYSTEM(78), has been set aside to indicate the use of piezoelectric materials. The default value for SYSTEM(78) is zero, implying that no piezoelectric materials are allowed. If SYSTEM(78) = 1, piezoelectric materials are allowed and coupling occurs between the structural and electrical degrees of freedom.

There are four BULK DATA cards that pertain specifically to piezoelectric modelling. MATPZ1 and MATPZ2 describe the piezoelectric material properties in two different ways. MATPZ1 is used to specify parameters for the permittivity constants

$[\epsilon]$, piezolectric constants $[d]$ and structural constants $[S^E]$ for an isotropic piezoelectric material, and MATPZ2 describes material constants for anisotropic materials.

2.4.4 NASTRAN(MSC) - The MacNeal-Schwendler Corp.

MSC-NASTRAN (The MacNeal-Schwendler Corp., 1990) does not contain structural piezoelectric modelling capabilitites in the same context as presented in the other commercial finite element codes. In other words, there are neither coupled-field finite elements as in ANSYS nor explicit piezoelectric structural elements as in ABAQUS.

2.4.5 Simulation Results

In order to assess the capabilities reported in the manuals for ANSYS and ABAQUS, the bimorph cantilevered beam proposed by Tzou (1987) has been selected. The objective here is to model this structure and compare the response by using the coupled-filed analysis in ANSYS and the piezoelectric elements in ABAQUS. The tip deflections due to an applied voltage of 1 V across the thickness are compared to the solutions obtained by the QUAD4-type (Venkayya and Tischler, 1992) plate formulation developed here.

The model developed for ANSYS consists of **SOLID5** elements, the three dimensional coupled-field solid elements. This element has eight nodes with four degrees of freedom per node (UX, UY, UZ, VOLT). The tip displacement predicted by ANSYS using solid brick elements was 3.45E-7 m, which agrees exactly with the tip displacement predicted by theory and the laminated plate theory. However, while only 5 plate type elements were used in the plate finite element model with 55 degrees of freedom, the ANSYS model required 100 solid brick type elements with 675 degrees of freedom.

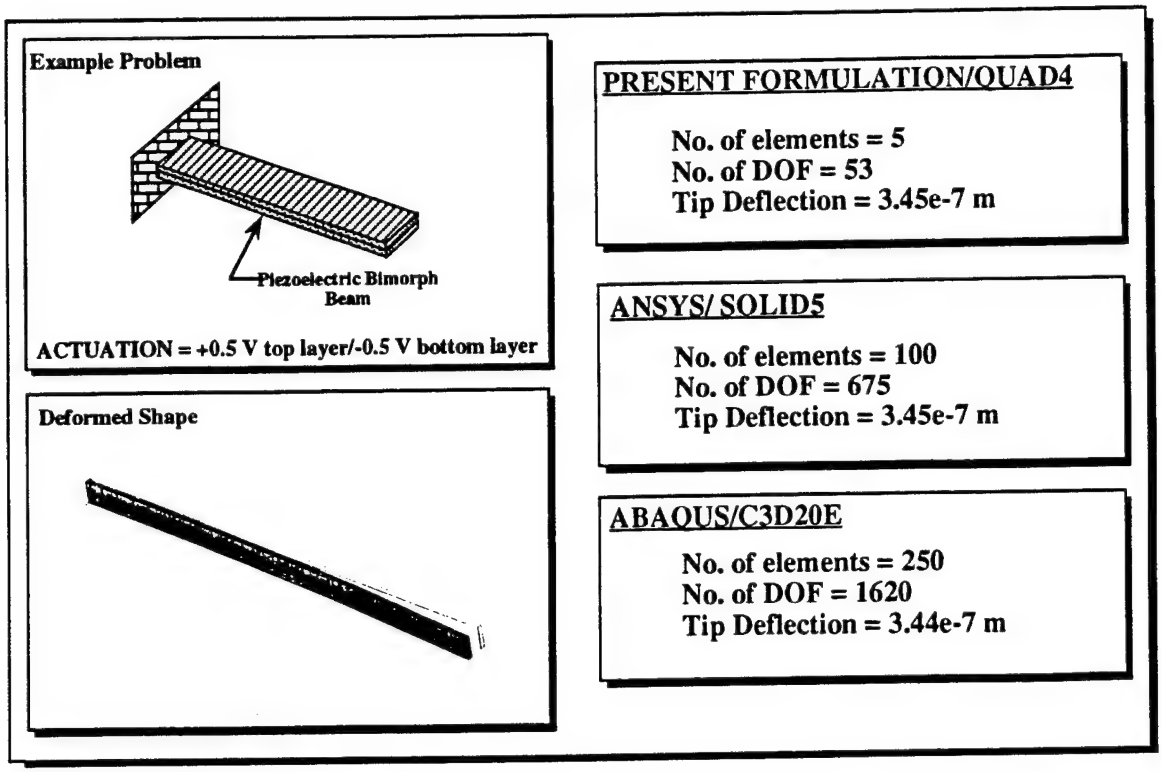

Figure 2-7 Comparison between the solid element models developed in ANSYS and ABAQUS and the composite plate element developed here.

In ABAQUS, the cantilevered plate was modelled using **C3D20E** elements. Since the elements developed in ABAQUS are based on a single point integration, more elements were required to model the structure. Here, 250 solid elements were used resulting in 1620 degrees of freedom. The tip deflection obtained due to the actuation of 1V was 3.44E-7 m.

Figure 2-7 shows the example problem used here, the deformed configuration in the presence of actuation and the tip deflection results for the three models for ANSYS, ABAQUS and laminated plate theory.

2.5 THERMAL ANALOGY

Since thermal and piezoelectric strains are both induced strains, the piezoelectric induced strains can be handled in the same manner as thermal strains. The piezoelectric material was assigned a coefficient of thermal expansion along with other material

properties such as Young's modulus. The combination of the thermal expansion coefficient multiplied by the change in temperature, the thermal strain, was set equal to the actuation strain of the piezoelectric material, i.e.

$$\alpha \Delta T = [d]\{E\}$$

where the piezoelectric strain is a combination of the piezoelectric constant $[d]$ multiplied by the electric field strength $\{E\}$.

Here, as an example, the same beam proposed by Tzou (1987) has been used. The thermal model was developed in ANSYS using **SOLID70** thermal elements. The thermal loads equivalent to the applied voltages resulted in a temperature distribution of $\pm 0.75°C$ along the top and bottom walls of the plate, and an applied temperature of $\pm 0.25°C$ along the inner walls (Figure 2-8). This is equivalent to applying a voltage differential of $+0.5V$ across the top layer and a voltage of $-0.5V$ across the bottom layer. It is observed that identical tip deflections are produced by both methods. It should be noted that the thermal loads can only be used in the context of actuation, as they are unable to simulate the converse effect found in piezoelectrics.

2.6 PRELIMINARY REMARKS

A new finite element formulation has been developed to analyze the electromechanical behaviour of laminated composite structures containing distributed piezoelectric actuators and sensors. This new Mindlin-type piezoelectric plate formulation has been implemented and its performance has been evaluated. Based on this study, the following remarks can be made:

(i) The numerical results generated by the electromechanical finite element plate model simulations agree well with experimental data and solid element formulations reported in the literature;

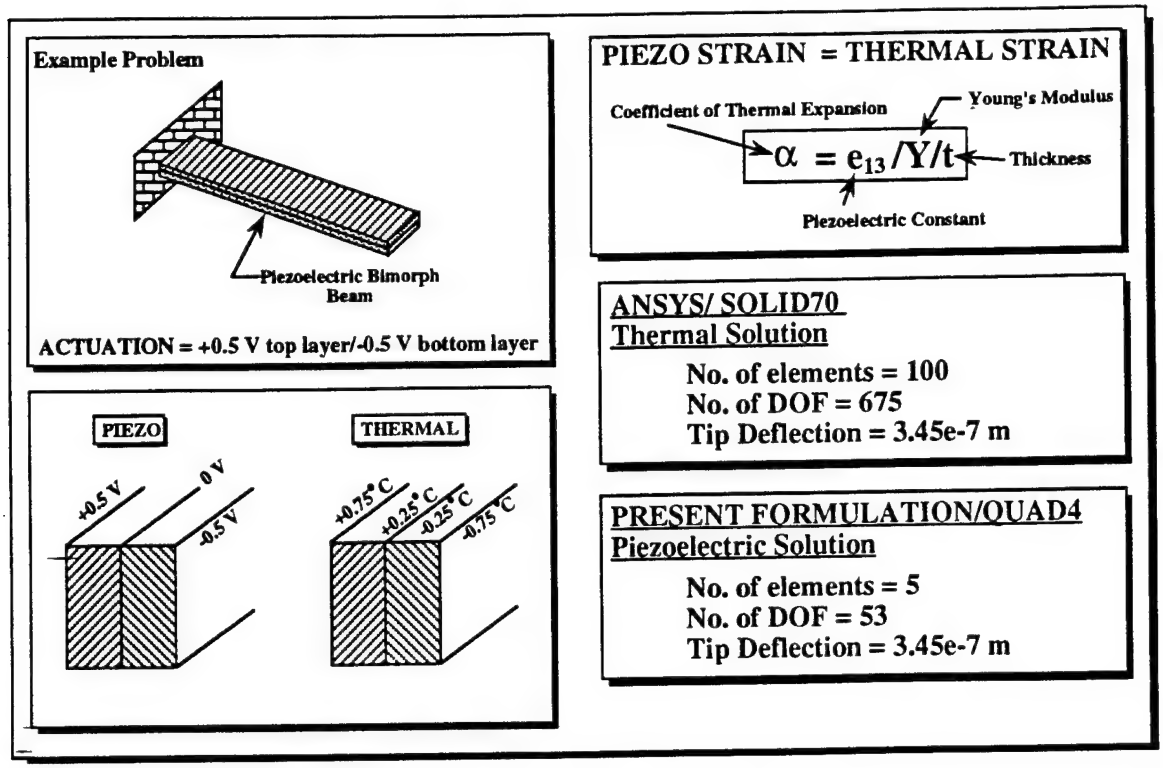

Figure 2-8 An example to establish the analogy between the thermal and piezoelectric behaviour.

(ii) the finite element model based on the Mindlin plate formulation with one electrical degree of freedom per piezoelectric layer is much simpler to formulate and more computationally efficient than models based on solid element formulations, where the number of degrees of freedom used to model the problem is significantly larger;

(ii) a few commercial finite element codes have the capability to model piezoelectric materials. However, only modelling using solid elements is available in these codes to the user resulting in models with a very large number of degrees of freedom, as demonstrated by an example;

(iv) the analogy between thermal and piezoelectric behaviour has been established by equating the thermal and piezoelectric strains.

CHAPTER
THREE

APPLICATION - FLUTTER CONTROL

Panel flutter is a self-excited, dynamic instability of thin plate or shell-like components of flight vehicles. It depends upon diverse factors such as Mach number, flow angle with respect to the panel, support conditions, curvature, in-plane stress and cavity effects, to name a few. It occurs most frequently in supersonic flow although, in subsonic flow, it can take the form of static divergence.

3.1 DESIGN PROBLEM

Consider a thin composite rectangular flat panel of length a, width b, and of uniform thickness h, mounted on a rigid wall as shown in Figure 3.1. The upper surface of the plate is exposed to a high supersonic airflow, at zero angle of attack and parallel to its side edges. Beneath the plate still air is present. In the presence of some disturbance, the plate can start to perform a perturbed motion with lateral deflection. We are interested in the study of the stability of such plate motion, called flutter, and investigate the feasibility of applying piezoelectric actuators to control it. Traditionally, these panels are designed for flutter by applying conventional methods of motion suppression such as thickening and reshaping the panels.

In adaptive structures research, considerable work has been carried out to investigate the feasibility of using piezoelectric materials to suppress vibration in structural systems. However, in the area of control of panel flutter, only a few research papers based on analytical solution methods have been reported (Scott and Weisshaar, 1991;

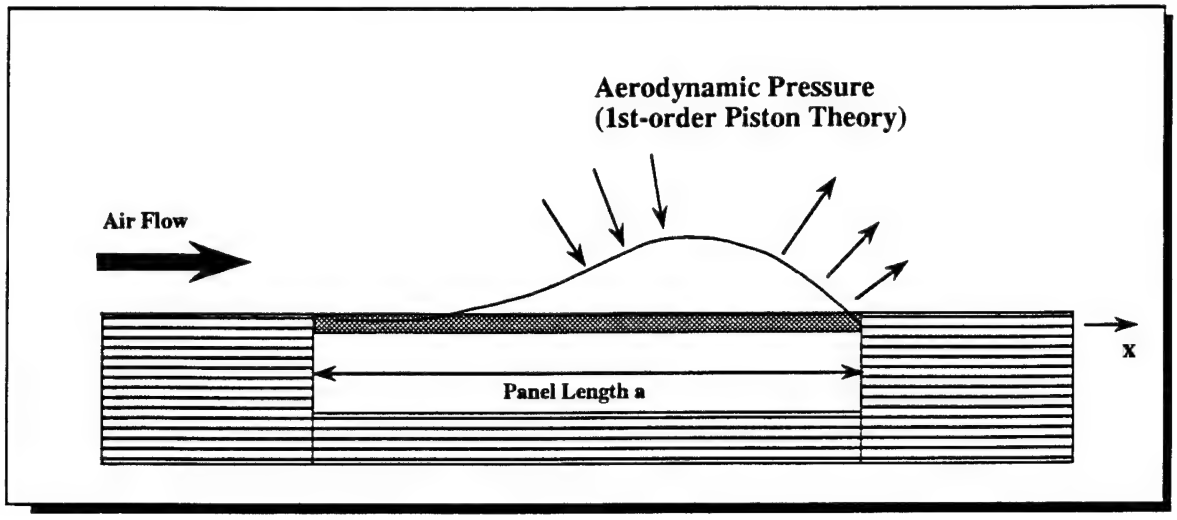

Figure 3.1 Self excited oscillations of an external panel of a flight vehicle exposed to supersonic air flow ($M > \sqrt{2}$)

Heeg, 1992; and Lai et. al., 1994).

Before attempting to use piezoelectric materials in panel flutter control problems, a knowledge of the degree of control authority exhibited by a typical piezoelectric actuator needs to be quantified.

Table 3.1 shows the material properties and operating conditions for a G1195 PZT piezoceramic. Relationships between the applied forces and the resultant responses depend upon the piezoelectric properties of the material, the size and shape of the patch and the direction of the electrical and mechanical excitation. For example, consider a typical piezoceramic patch with dimensions $5 \times 5 \times 0.05$ cm. The stress free length change in the in-plane direction can be expressed as $\Delta L = d_{31}Ea = 6.6\mu m$, where E, the electrical field, is the applied voltage per unit length. The strain free force in the in-plane direction due to an applied voltage of 400 V is $F = Yd_{31}Ebh = 200$ N. Table 3-2 shows the actuation capabilities and the power requirements for an applied voltage of 400 V at 10 Hz.

The question that needs to be raised now is the piezoceramic patch capable of

Table 3-1 Material properties and operating conditions for a G1195 PZT piezoceramic.

PIEZOCERAMIC - G1195		
Piezoelectric Charge Coefficient (d31)	**= 166**	**pm/V**
Eleastic Modulus (Y)	**= 63**	**GN/m^2**
Capacitance (C)	**= 90**	**nF**
Curie Temperature	**= 360**	**^oC**
Maximum Electrical Field (E)	**= 2.0**	**MV/m**
Density	**= 7650**	**Kg/m^3**

generating a significant force output in order to affect the stiffness of the panel, and thus push back the flutter boundary envelope. Figure 3-2 shows the effect that in-plane loads have on the flutter boundary. Tensile loading, which can be generated by piezoelectric actuators, causes the flutter boundary to shift considerably. For example, for a simply-supported panel with dimensions $30 \times 30 \times 0.1$ cm, the range of in-plane force that affects the coalescence of the first mode lies in the 200 to 2,000 N range (Nasr-Bismarck, 1992). Therefore, it can be inferred that an arrangement of piezoelectric patches where each exerts an in-plane force of approximately 200 N, due to an applied voltage of 400 V, is capable of significantly affecting the panel flutter characteristics.

Table 3-2 The actuation capabilities and power requirements for a typical piezoceramic patch.

CAPABILITIES AND REQUIREMENTS		
Piezoceramic Patch	**= 5.0 x 5.0 x 0.05**	**cm**
Stress Free Length Change	**= 6.6**	**μ m**
Strain Free Force	**= 200**	**N**
Moment Generated	**= 0.3**	**Nm**
Electrical Current	**= 2.0**	**mA**
Electrical Power	**= 1.0**	**W**
Electrical Charge	**= 36**	**μ C**

3.2 PANEL FLUTTER MODEL

In the supersonic regime, above a Mach number of about $\sqrt{2}$, simple approximations for the aerodynamic forces such as piston theory, give satisfactory results (Bisplinghoff, Ashley and Halfman, 1955).

3.2.1 First Order Piston Theory

Piston theory gives the following simple relation between pressure and motion (Bismarck-Nasr, 1992)

$$\Delta p = \rho_\infty a [\frac{\partial w}{\partial t} + U_\infty \frac{\partial w}{\partial x}]. \tag{3.1}$$

In the above relation we assume that the deflection is zero at the panel's leading and trailing edges. The work done by the aerodynamic surface pressure can be calculated

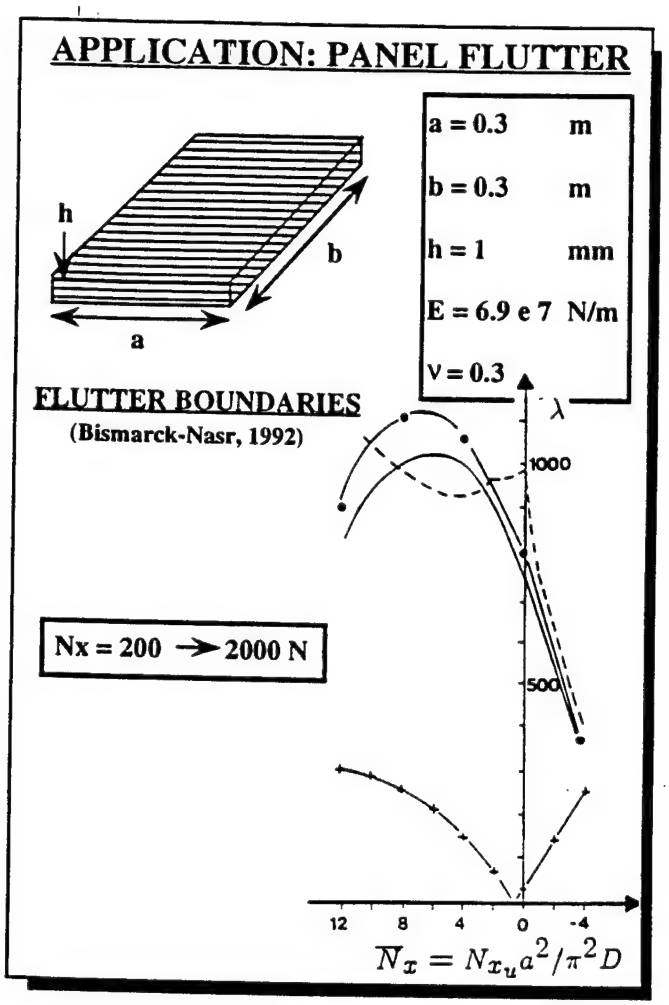

Figure 3.2 Effect of in-plane tensile forces

by the principle of virtual work:

$$W = -\int_A \frac{2Q}{V\beta}\left(V\frac{\partial w}{\partial x} + \frac{M^2-2}{M^2-1}\frac{\partial w}{\partial t}\right) w dA \tag{3.2}$$

where $Q = \rho V^2/2$ is the free stream dynamic pressure, $\beta = \sqrt{M^2-1}$, V is the free stream velocity, M is the free stream Mach number, and ρ_∞ is the air density.

Substituting Equation (3.2) into Hamilton's equation, we obtain the following aerodynamic damping and stiffness matrices for each element:

$$\mathbf{A}_1^{\mathbf{j}} = g\int_A \mathbf{N}^T\mathbf{N} dA, \qquad j = 1, \ldots, n_{el};$$

$$\mathbf{A_2^j} = \lambda \int_A \mathbf{N}^T \mathbf{N}_{,\mathbf{x}} dA, \qquad j = 1, \ldots, n_{el};$$

and

$$g = \frac{2Q(M^2 - 2)}{V(M^2 - 1)^{\frac{3}{2}}}; \qquad \lambda = \frac{2Q}{(M^2 - 1)^{\frac{1}{2}}}$$

where g is the aerodynamic damping constant and λ is the dynamic presure parameter. The aerodynamic damping matrix is proportional to the mass matrix and is given by

$$\mathbf{A}_1^j = \frac{\mathbf{M}_{cc}^j}{\rho}, \qquad j = 1, \ldots, n_{el}$$

where ρ is the material mass density. The aerodynamic stiffness matrix $\mathbf{A}_2^j$ is nonsymmetric, due to the nonconservative nature of the aerodynamic loading.

3.2.2 The Effect of Initial Pre-Stresses

The effect of inplane stresses is particularly important since passive control can be achieved by the inplane stresses generated by the piezoelectric layers in the composite plate. It will be assumed that the panel has reached a state of equilibrium due to the presence of the initial stresses, and the stability of the system will be examined at that position. It is also assumed that the panel has not reached a buckled state. The inplane initial stresses N_x, N_y and N_{xy} are forces per unit distance and are assumed constant and positive, as shown in Figure 3.3. Again Hamilton's principle will be used in order to formulate the problem. Thus

$$\int_{t_0}^{t_1} \delta(T - U - U_i) dt = 0$$

Here, the strain energy due to the pre-stresses is given by

$$U_i = \frac{1}{2} \int_A \left[N_x \left(\frac{\partial w}{\partial x}\right)^2 + N_y \left(\frac{\partial w}{\partial y}\right)^2 + N_{xy} \frac{\partial w}{\partial x} \frac{\partial w}{\partial y} \right] dA \tag{3.3}$$

Substituting, integrating and minimizing, we obtain for each element the following

geometric stiffness matrix:

$$\mathbf{K}_g^j = N_x \int_A \mathbf{N}, \mathbf{x}^T \mathbf{N}, \mathbf{x} dA + N_y \int_A \mathbf{N}, \mathbf{y}^T \mathbf{N}, \mathbf{y} dA$$
$$+ N_{xy} \int_A \mathbf{N}, \mathbf{x}^T \mathbf{N}, \mathbf{y} dA + N_{xy} \int_A \mathbf{N}, \mathbf{y}^T \mathbf{N}, \mathbf{x} dA; \qquad j = 1, ..., n_{el} \quad (3.4)$$

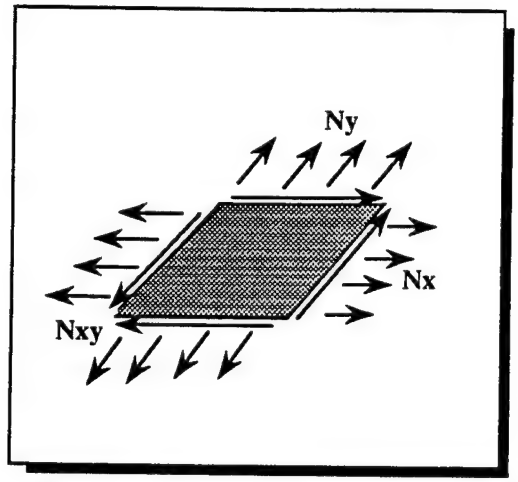

Figure 3.3 Initial in-plane pre-stresses on the panel due to piezoelectric actuation.

3.2.3 Equations of Motion

For the entire structure, using the standard assembly technique for the finite element method and applying the appropriate boundary conditions, we obtain the equations of motion for a composite panel with piezoelectric layers in a supersonic flow field

$$\overbrace{\begin{bmatrix} \mathbf{M}_{cc} & \mathbf{0} \\ \mathbf{0} & \mathbf{0} \end{bmatrix}}^{Inertia} \begin{Bmatrix} \ddot{\bar{U}}^c \\ \ddot{\bar{U}}^e \end{Bmatrix} + \overbrace{\begin{bmatrix} \mathbf{K}_{cc} & \mathbf{0} \\ \mathbf{0} & \mathbf{0} \end{bmatrix}}^{Elastic\ Stiffness} \begin{Bmatrix} \bar{U}^c \\ \bar{U}^e \end{Bmatrix} + \overbrace{\begin{bmatrix} \mathbf{A}_1 & \mathbf{0} \\ \mathbf{0} & \mathbf{0} \end{bmatrix}}^{Aero\ Damping} \begin{Bmatrix} \dot{\bar{U}}^c \\ \dot{\bar{U}}^e \end{Bmatrix} +$$

$$\overbrace{\begin{bmatrix} \mathbf{A}_2 & \mathbf{0} \\ \mathbf{0} & \mathbf{0} \end{bmatrix}}^{Aero\ Stiffness} \begin{Bmatrix} \bar{U}^c \\ \bar{U}^e \end{Bmatrix} + \overbrace{\begin{bmatrix} \mathbf{0} & \mathbf{K}_{ce} \\ \mathbf{K}_{ec} & \mathbf{K}_{ee} \end{bmatrix}}^{Piezo\ Stiffness} \begin{Bmatrix} \bar{U}^c \\ \bar{U}^e \end{Bmatrix} + \overbrace{\begin{bmatrix} \mathbf{K}_g & \mathbf{0} \\ \mathbf{0} & \mathbf{0} \end{bmatrix}}^{Geometric\ Stiffness} \begin{Bmatrix} \bar{U}^c \\ \bar{U}^e \end{Bmatrix} = \mathbf{0}$$

3.3 PASSIVE CONTROL

First, let us examine the development of flutter in the panel, in the absence of any piezolectric actuation. The panel, made of aluminum with the properties as shown in Figure 3-2, is simply supported along all four of its sides. Sixty-four finite elements with 309 structural degrees of freedom are used to model the plate. As the dynamic pressure increases, the natural frequencies of the first and second modes get closer (Figure 3-4), until they coalesce, and the dynamic pressure λ at this point is called the critical dynamic pressure. For this particular panel, neglecting the aerodynamic damping effect, the critical dynamic pressure parameter is 38.8 psi. After coalescence of the first two modes, the imaginary parts of the eigenvalues become split, one towards the negative side, and the other towards the positive side. When λ passes the critical point, the system becomes inherently unstable, such that a small disturbance makes the amplitude of the panel deflection diverge. As λ increases further, the third and fourth modes coalesce as well. The fundamental mode shape in a vacuum and following the onset of flutter is also shown in Figure 3-4.

Using the passive control methodology, the flutter velocity of panels, or similarly the critical dynamic pressure, can be increased by making piezoelectric actuators induce in-plane tensile forces which alter the effective stiffness of the panel. This strategy is depicted in Table 3-3. The same voltage is applied to the the top and bottom piezoelectric layers, resulting in uniform compression or tension in the plate. This static loading condition on the panel induces in-plane stresses N_x, N_y and N_{xy}. These stresses are subsequently used to calculate the geometric stiffness of the plate, which couples the in-plane and transverse motions of the panel. Subsequently, the geometric stiffness matrix is added to the linear stiffness matrix, and the eigenvalue problem is solved. The value for λ at which a complex solution exists is considered to

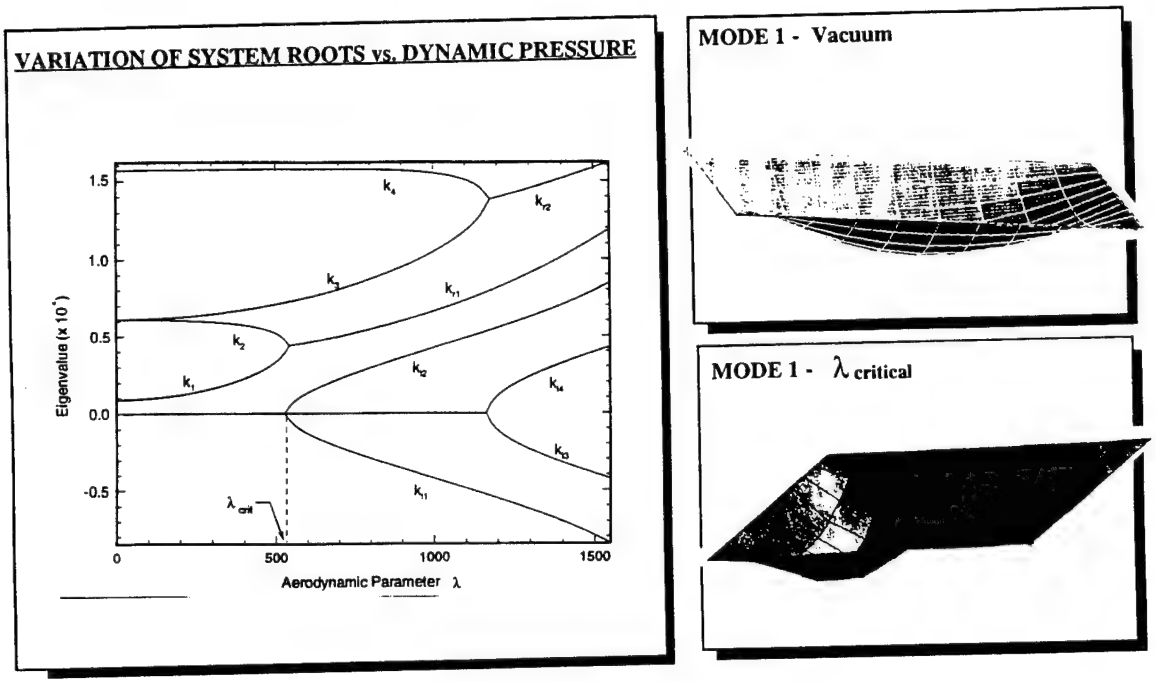

Figure 3.4 The natural frequencies solution as a function of dynamic pressure. The fundamental mode shapes are shown in vacuum and following the onset of flutter.

be the onset of flutter. When the piezoelectric patches create a state of tension in the panel, the dynamic pressure increases. If the piezoelectric patches exert compressive forces on the panel, the dynamic pressure decreases.

Now, let us examine a passive actuation configuration in which the piezoelectric patches cover the center of the plate (Figure 3-5). First, consider a case where the patches cover only 6% of the plate area. Here, the mass increases by 17% due to the addition of the piezo patches to the base structure. Obviously, the effective stiffness also increases. It was observed that the critical dynamic pressure increased from 36.8 to 46.9, an improvement of 27%. Note that this increase is solely due to the bonding of the piezo patches to the top and bottom surfaces of the aluminum

Table 3-3 Passive control methodology flowchart.

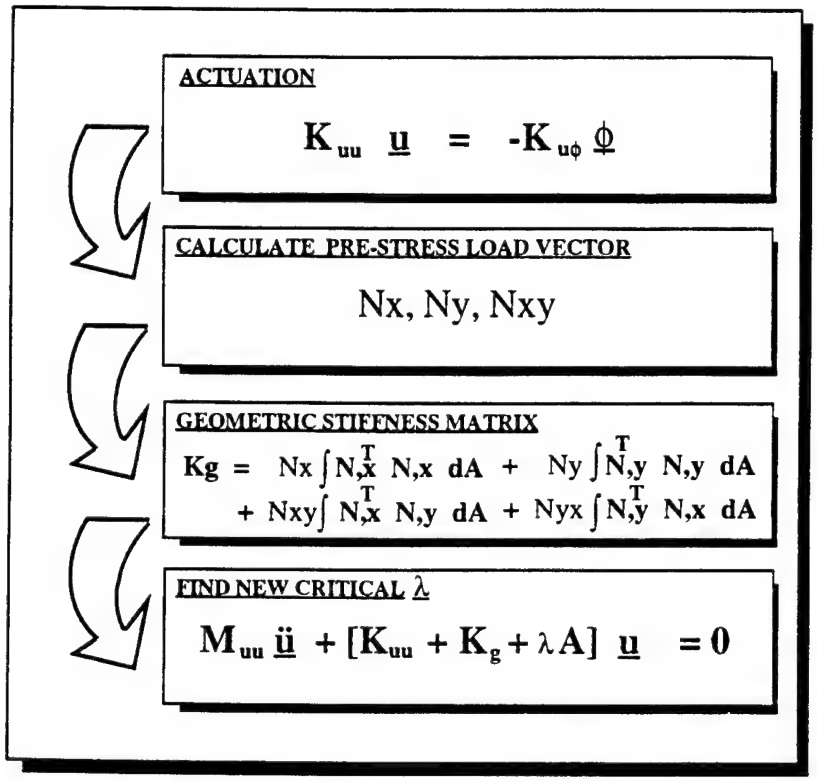

panel. Subsequently, the piezo patches were actuated with a voltage of 400 V and, in this instance, a further increase of 42% was attained, relative to the case where no voltage was applied. Summarizing, a better performance was indeed attained by the piezoelectric actuation. The effective stiffness was increased by merely attaching the piezo patches in the first instance, and a further increase was obtained by actuating the piezo patches with an applied voltage.

Next, the performance of a patch which covered 25% of the plate area was assessed. Here, a substantial increase in mass was observed (69%). The addition of piezo patches with no voltage applied resulted in an increase of 92% in dynamic pressure. Further application of 400 V across each layer resulted in a smaller further

improvement in dynamic pressure to 93.5, or 32% relative to the 0 V case. Thus, it is noted that an increase in size of the piezo patches and/or actuation power, does not necessarily result in better performance. In fact, the 25% patch configuration performed worse than the 6% patch case. Apparently, the larger piezo patch configuration resulted in a relatively much larger mass increase thus offsetting the benefits of an increased actuation capability.

Three more patch configurations have been analyzed to further probe this matter. Let us call these configurations 1, 2 and 3, as shown in Figure 3.6. In configuration 1, five piezo patches are placed in a star shaped form, resulting in a mass increase of 86%. The flutter dynamic pressure, in the presence of an applied voltage of 400 V, exhibits a poor performance with a mere 5% increase in value relative to the no applied voltage case. In other words, a larger actuation capability, followed by a much larger mass increase resulted in a negligible improvement. For configuration 2, with 4 piezoelectric patches arranged in a cross shape, the mass increased by 69%. The resultant critical dynamic pressure increased by 8% to 99.2 due to an applied voltage of 400 V. Finally, configuration 3 with the piezo patches arranged along the perimeter of a square at the centre of the plate, exhibited an increase of 20% in dynamic pressure, with an increase of 52% in mass. Thus, in configuration 3, a better performance was attained in the presence of a relatively smaller increase in mass, while in configuration 1, a poor performance was exhibited with a substantial increase in mass.

Another aspect that draws attention is the fact that the 25% central patch configuration and the number 2 configuration provide a similar mass increase (69%). However, the 25% central patch configuration resulted in a 32% improvement in dynamic pressure, while the actuation in configuration 2 exhibited a poor 8% improvement. On a preliminary analysis basis, it can be inferred that not only is the added mass to

stiffness ratio important, but also the configuration and placement of the patches on the structure should be taken into account during the design process.

Summarizing, there is an optimum patch size, and there in an optimal patch configuration which deliver the best performance. A compromise needs to be found between the advantages of an increased actuation capability and the disadvantages of an increased weight due to the addition of piezoelectric material. These questions need to be addressed through formal optimization design procedures.

3.4 PRELIMINARY REMARKS

The feasibility of employing piezoelectric actuators to control panel flutter is investigated. The panel is an aluminum simply supported plate with piezoelectric patches bonded to the top and botton walls of the structure, in various configurations.

Here, a passive control methodology is proposed, where the top and bottom layers are subjected to identical voltages. The actuation stiffens the plate. Based on the simulations, the following can be inferred:

(i) Flutter control using piezoceramics is dependent on the mass to stiffness ratio and on the configuration and placement of the patches;

(ii) the application of piezoceramics as actuation devices in panel flutter problems may be limited by its high material density; and

(iii) formal optimization design procedures need to be invoked in order to address the issue of optimal actuator size, shape and placement.

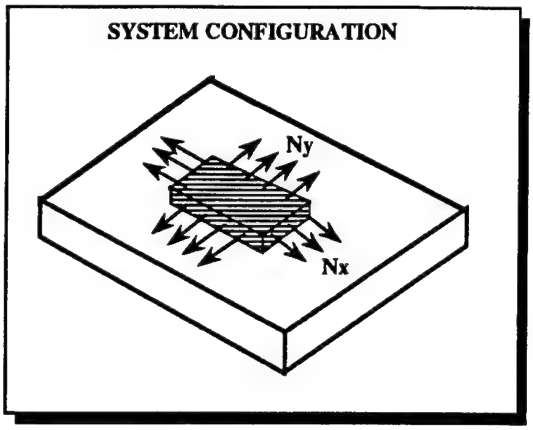

Critical Aerodynamic Parameter
(Aluminum Panel Substructre)

$\lambda_{crit} = 36.8$

$\overline{\lambda}_{crit} = \lambda_{crit}\ a^3/D = 512$

	Critical Aerodynamic Parameter λ_{crit}	
Applied Voltage	6% Patch	25% Patch
0 V	46.9	70.5
200 V	57.0 (21%)	81.6 (16%)
400 V	66.7 (42%)	93.5 (32%)
Mass	+17%	+69%

Figure 3.5 Critical dynamic pressure results for a central piezoelectric patch configuration for two sizes of actuation capabilities.

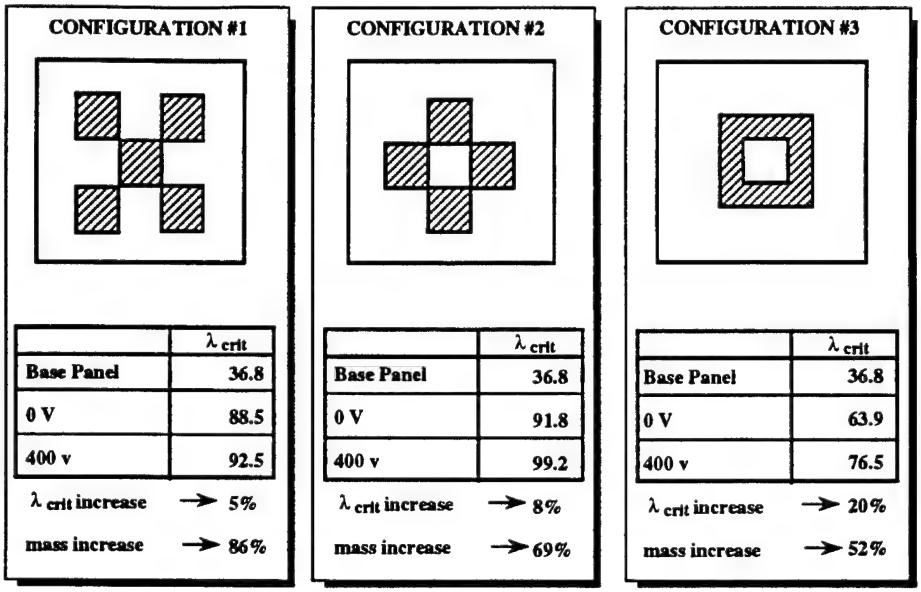

	λ_{crit}
Base Panel	36.8
0 V	88.5
400 v	92.5

λ_{crit} increase → 5%

mass increase → 86%

	λ_{crit}
Base Panel	36.8
0 V	91.8
400 v	99.2

λ_{crit} increase → 8%

mass increase → 69%

	λ_{crit}
Base Panel	36.8
0 V	63.9
400 v	76.5

λ_{crit} increase → 20%

mass increase → 52%

Figure 3.6 Critical dynamic pressure results for three different patch configurations.

CHAPTER
FOUR

CONCLUDING REMARKS

The possibility of employing adaptive materials to control panel flutter has been considered. First, a simple finite element formulation for a composite plate with laminated piezoelectric layers is presented. Classical laminate theory with electromechanical induced actuation and sensing and variational principles are used to formulate the equations for a Mindlin plate finite element based upon uniformly reduced integration and hourglass stabilization. The equations of motion are discretized with four node, 24 degree of freedom quadrilateral shell elements with one electrical degree of freedom per piezoelectric layer. Based on this study, the following remarks can be made:

(i) The numerical results generated by the simple and efficient finite element developed here agree well with experimental data and solid element formulations reported in the literature;

(ii) the finite element model based on the single point integration Mindlin plate formulation and one electrical degree of freedom per piezoelectric layer is much simpler to formulate and more computationally efficient than models based on solid element formulations, where the number of degrees of freedom used to model the problem is significantly larger.

Next, the feasibility of employing the piezoelectric effect to control panel flutter is investigated. The panel is an aluminum simply supported plate with piezoelectric patches bonded to the top and bottom walls of the structure, in various configurations.

Here, a passive control methodology is proposed, where the top and bottom piezoelectric patches are subjected to identical voltages. The actuation voltage contracts the plate, stiffening it. The resultant stresses are used to calculate the geometric stiffness matrix. Based on the simulations, the following can be inferred:

(i) The critical aerodynamic parameter, defined as the value at which the eigenvalues become complex, increases considerably due to the added mass of the piezoelectric patches. However, a maximum 42% increase in the aerodynamic parameter was attained due to an applied voltage of 400 V at the top and bottom layers in a patch which covered 6% of the plate area.

(ii) It was further observed that flutter control is dependent on the mass to stiffness ratio, and on the placement and configuration of the piezoelectric patches.

(iii) The application of piezoceramic materials as actuator devices in panel flutter problems may be limited by the material high density.

(iv) Formal optimization design procedures need to be invoked to address the issue of optimum actuator size and placement in order to attain optimal performance.

Anders, W.S., Rogers, C.A., 1990, "Vibration and Low Frequency Acoustic Analysis of Piecewise Activated Adaptive Composite Panels", *1st Joint US-Japan Conference on Adaptive Structures*, Maui, Hawaii, USA:285-303.

Belvin W.K., Edighoffer, H.H., and Herstrom, C.L., 1989, "Quasistatic Shape Adjustment of a 15-meter Diameter Space Antenna", *Journal of Spacecraft*, **26**(3):129-136.

Belytschko, T., Lin, J.I., and Tsai, C.S., 1984, "Explicit Algorithms for the Nonlinear Dynamics of Shells", *Comp. Meth. Appl. Mech. Engng.*, **42**:225-251.

Belytschko, T., Tsay, C.S., and Lin, J.I., 1981, "A Stabilization Matrix for the Bilinear Mindlin Plate Element", *Comp. Meth. Appl. Mech. Engng.*, **29**:313-327.

Belytschko, T., and Tsay, C.S., 1983, "A Stabilization Procedure for the Quadrilateral Plate Element with One-point Quadrature", *Int. J. Num. Meth. Engng.*, **19**:405-419.

Bisplinghoff, R.L., Ashley H., and Halfman, R.L., 1955, "Aeroelasticity", Addison-Wesley Publishing Co.

Breitbach, E.J., 1991, "Research Status on Adaptive Structures in Europe", Second Joint Japan-US Conference on Adaptive Structures", Nagoya, Japan, 32-48.

Brockman, R.A., Lung, F.Y., and Braisted, W.R., 1989, "Probabilistic Finite Element Analysis of Dynamic Structural Response", *Air Force Wright Aeronautical Laboratories*, AFWAL-TR-88-2149.

Crawley, E.F., and de Luis, J., 1985, "Use of Piezoceramic as Distributed Actuators in Large Space Structures", *Proceedings of the AIAA/ASME/ASCE 26th Structures, Structural Dynamics, and Materials Conference*, Part 2:126-133.

Crawley, E.F., and de Luis, J., 1991, "Experimental Verification of Piezoelectric Actuators for Use in Precision Space Structures", AIAA Paper No. 83-0878.

Crawley, E.F., and Lazarus, K.B., 1991, "Induced Strain Actuation of Isotropic and Anisotropic Plates", *AIAA Journal*, **29**(6):944-951.

Elhers, S.M., and Weisshaar, T.A., 1990, "Static Aeroelastic Behaviour of an Adaptive Laminated Piezoelectric Composite Wing", *Proceedings of the 31st Structures, Dynamics and Materials Conference*, Long Beach, CA.

Flanagan, D., and Belytschko, T., 1981, "A Uniform Strain Hexahedron and Quadrilateral with Orthogonal Hourglass Control", *Int. J. Num. Meth. Engng.*, **17**:679-706.

Gardiner, P, Culshaw, B., McDonach A., Michie, C., Pethrick, R., 1991, "Smart Structures Research Institute - Activities, Plans and Progress", *2nd Joint Japan-US Conference on Adaptive Structures*, Nagoya, Japan:49-58.

Ha, S.K., Keilers, C., and Chang, F.-K., 1992, "Finite Element Analysis of Composite Structures Containing Distributed Piezoceramic Sensors and Actuators" *AIAA Journal*, **30**(3):772-780.

Hall, S.R., Crawley, E.F., How, J.P., Ward, B., 1991, "Hierarchic Control Architecture for Intelligent Structures", *J. of Guidance, Control, and Dynamics*, **14**(3):503-512.

Heeg, J., 1992, "An Analytical and Experimental Investigation of Flutter Suppression via Piezoelectric Actuation", *Proceedings of the AIAA Dynamics Specialist Conference*, Dallas, TX:237-247.

Hollkamp, J.J., 1994, "Multimodal Passive Vibration Suppression with Piezoelectric Materials and Resonant Shunts". *J. Intel. Mat. Sys. and Struct.*, **5**(1):49-57.

Hughes, T.J.R., Cohen, M., and Haroun, M., 1978, "Reduced and Selective Integration Techniques in Finite Element Analysis of Plates", *Nucl. Eng. Des.*, **46**:203-222.

Hughes, T.J.R., Tezduyar, T.E., 1981, "Finite Elements Based upon Mindlin Plate Theory with Particular Reference to the Four-Node Bilinear Isoparametric Element", *J. Appl. Mech.*, **48**:587-596.

Jones, R.M., 1975, *Mechanics of Composite Materials*, Scripta Book Co., Washington, D.C.

Kosloff, D., and Frazier, G., 1978, "Treatment of Hourglass Patterns in Low Order Finite Element Codes", *Num. Anal. Meth. Geomech.*, **2**:52-72.

Lai, Z., Xue, D.Y., Huang, J.-K., and Mei, C., 1994, "Nonlinear Panel Flutter Suppression with Piezoelectric Actuation", paper submitted to *J. Intel. Mat. Sys. and Struct.*

Lazarus, K.B. and Napolitano, K.L., 1993, "Smart Structures, an Overview", *Wright Laboratory*, Report No. WL-TR-93-3101.

Lazarus, K.B., Crawley, E.F., and Bohlman, J.D., 1990, "Static Aeroelastic Control Using Strain Actuated Adaptive Structures", *1st Joint US-Japan Conference on Adaptive Structures*, Hawaii, USA:197-226.

Lee, C.K., 1990, "Theory of Laminated Piezoelectric Plates for the Design of Distributed Sensors/Actuators. Part I: Governing Equations and Reciprocal Relationships", *J. Acoust. Soc. Am.*, **87**(3):1144-1158.

Lin, R.R., 1990, "Active Vibration Control of Rotorbearing Systems Utilizing Piezoelectric Pushers", Ph.D. Dissertation, Texas A & M University.

MacNeal, R.H., 1978, "A Simple Quadrilateral Shell Element", *Comp. Struct.*, **8**:175-183.

Matsubara, T., Yamamoto, H., Misumoto, H., 1989, "Chatter Suppression by Using Piezoelectric Active Dampers", *Rotary Machinery Dynamics*, **DE-18-1**:79-83.

Mindlin, R.D., 1951, "Influence of Rotary Inertia and Shear on the Bending of Elastic Plates", *J. Appl. Mech*, **18**:1031-1036.

Miura, K., Natori, M.C., 1991, "Aerospace Research Status on Adaptive Structures in Japan", *2nd Joint Japan-US Conference on Adaptive Structures*, Nagoya, Japan:3-14.

Mitsugi, J., Yasaka, T., Miura, K., 1990, "Shape Control of Tension Truss Antenna", *AIAA Journal*, **28**(2):316-322.

Nasr-Bismarck, M.N., 1992, "Finite Element Analysis of Aeroelasticity of Plates and Shells", *Appl. Mech. Rev.*, **45**(12):461-482.

Natori, M., Murohashi, S., Takahara, K., and Kuwao F., 1989, "Control of Truss Structures Using Member Actuators with Latch Mechanism", *The Winter Annual Meeting of the ASME*, San Francisco, CA:69-75.

Palazzolo, A.B., Lin, R.R., Kascak, A.F., Montague, J., Alexander, R.M., 1989, "Piezoelectric Pushers for Active Vibration Control of Rotating Machinery", *ASME Journal of Vibration, Acoustics, Stress, and Reliability in Design*, **111**:298-305.

Park, K.C., Stanley, G.M., Flaggs, D.L., 1985, "A Uniformly Reduced, Fournoded C^0 Shell Element with Consistent Rank Corrections", *Comp. Struct.*, **20**:129-139.

Scott, R.C., and Weisshaar, T.A., 1991, "Controlling Panel Flutter Using Adaptive Materials", *Proceedings of the 32nd Structures, Structural Dynamics, and Materials Conference*, Baltimire, MD:2218-2229.

Tabata, M., Yamamoto, K., Inoue, T., Noda, T., Miura, K.,1991, "Shape Adjustment of a Flexible Space Antenna Reflector", *2nd Joint Japan-US Conference on Adaptive Structures*, Nagoya, Japan: 393-405.

Taylor, R.L., 1979, "Finite Element for General Shell Analysis", *5th Intl. Seminar on Computational Aspects of the Finite Element Method*, Berlin.

Tzou, H.S., 1987, "Active Vibration Control of Flexible Structures via Converse Piezoelectricity", *Developments in Mechanics*, **14-c**:1201-1206.

Tzou, H.S., and Gadre, M., 1989, "Theoretical Analysis of a Multi-layered Thin Shell with Piezoelectric Shell Actuators for Distributed Vibration Controls" *Journal of Sound and Vibration*, **132**:433-450.

Tzou, H.S., and Tseng, C.I., 1990, "Distributed Piezoelectric Sensor/Actuator Design for Dynamic Measurement/Control of Distributed Parameter Systems: a Piezoelectric Finite Element Approach", *Journal of Sound and Vibration*, **138**(1):17-34.

Venkayya, V.B., and Tischler, V.A., 1989, "QUAD4 Seminar" *Wright Research and Development Center*, WRDC-TR-89-3046.

Wada, B.K., 1991, "Application of Adaptive Structures for the Control of Truss Structures", *2nd Joint Japan-US Conference on Adaptive Structures*, Nagoya, Japan:123-131.

Wang, B.T., and Rogers, C.A., 1991, "Modelling of Finite-Length Spatially Distributed Induced Strain Actuators for Laminate Beams and Plates", *J. Intel. Mat. Sys. and Struct.*, **2**(1):38-58.

Whitney, J.M., 1973, "Shear Correction Factors for Orthotropic laminates under Static Load", *J. Appl. Mech.*, **40**:302-304.

Zienkiewicz, O.C., 1977, *The Finite Element Method*, McGraw-Hill Co., New York.

APPENDIX
ONE

PROGRAM INPUT DATA

The computer program used in this analysis to implement the piezoelectric and flutter analysis capabilities is PROTEC (Brockman, 1989). Here, additional input data to simulate the piezoelectric actuation and sensing, panel flutter and passive control are explained.

Input to PROTEC is arranged in a series of input blocks. Each block begins with a header line identifying the block, followed by the data, and ends with a blank signifying the end of the block. The following input blocks have been modified or added to the input data descriptions:

Table A-1 Changes and additional input blocks and data descriptions incorporated into PROTEC.

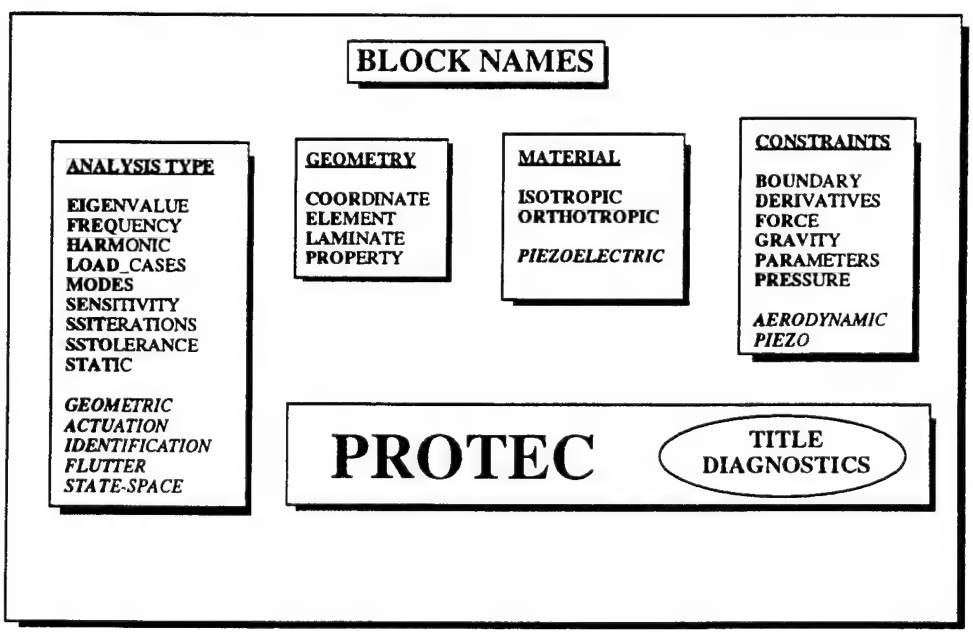

AERODYNAMIC Input block: Aerodynamic dynamic pressure for flutter analysis.

Header: **AERO**
Format:

(1) For flutter analysis to find critical dynamic pressure

10	20	30	40
LAM0	LAMF	INC	CONST

Variables:

LAM0	Initial guess for critical dynamic pressure
LAMF	Final guess for critical dynamic pressure
INC	Incremental step during iteration
CONST	Non-dimensionalizing parameter a**3/D
D	Bending rigidity of plate
a	Plate length

MATERIAL Input block: Material properties data for piezoelectrics.

Header: <u>MATE</u>
Format:

(1) For isotropic materials (one line/material)

5	10	20	30	40	50
MAT		E	XNU	RHO	SY

(2) For orthotropic materials (two lines/material)

5	10	20	30	40	50
MAT		E1	E2	XNU12	G12
		RHO	C1	C2	

60	70
G13	G23

(2) For piezoelectric materials use the isotropic/orthotropic options together with the piezoelectric constant D31, D32, D33, EPSI or E31, E32, EPSI

80	90	100	110
E31/D31	E32/D32	EPSI/D33	0/EPSI

Variables:

MAT	Material number for current material
E	Extensional modulus
XNU	Poisson's ratio
SY	Mass density
E1	Extensional modulus in direction 1
E2	Extensional modulus in direction 2
XNU12	Major inplane poisson's ratio
G12	Shear modulus in (1,2) plane
G13	Shear modulus in (1,3) plane
G23	Shear modulus in (2,3) plane
C1,C2	Failure stress constants
E31,E32	Piezoelectric constants at constant strain
D31,D32,D33	Piezoelectric constants at constant stress
EPSI	Dielectric material constant

OPTION Input block: Selection of solution options.

Header: <u>OPTI</u>
Format: Free

Examples:

```
OPTION
GEOMETRIC
STATIC
FLUTTER
```

Options:

EIGENVALUE	Selects natural frequencies solution.
FREQUENCY <name>	Defines forcing frequencies for steady-state harmonic solution.
HARMONIC	Selects steady-state forced harmonic vibration solution.
LOAD_CASES	Defines number of static loading cases.
MODES	Requests a specified number of natural frequencies in an eigenvalue analysis.
SENSITIVITY <name>	Requests sensitivity analysis following a basic solution, to determine response derivatives.
SSITERATIONS	Defines the maximum number of iteration cycles for eigenvalue solutions.
SSTOLERANCE	Defines the relative accuracy tolerance to test eigenvalue convergence.
STATIC	Selects linear static solution.

<u>NEW IMPLEMENTATIONS:</u>

GEOMETRIC	Calculates the nonlinear geometric matrix due to piezoelectric actuation.
ACTUATION	Calculates the displacement solution due to piezoelectric actuation.
IDENTIFICATION	Calculates the sensing voltages due to an applied mechanical force or prescribed displacement field.
FLUTTER	Calculates the critical aerodynamic parameter at onset of flutter.
STATE-SPACE	Calculates the control system matrix [A,B,C,D] for input to MATLAB.

Notes:

1. The GEOMETRIC solution requires piezoelectric actuation in oeder to calculate the nonlinear stiffness matrix Kg.
2. FLUTTER solution requires the AERODYNAMIC block in order to iterate within a range to find the critical aerdynamic parameter.
3. ACTUATION requires the PIEZO block in order to specify the actuation voltages.

PIEZO Input block: Actuation voltages per piezoelectric layer.

Header: **PIEZ**
Format:

(1) To apply actuation voltages to the piezoelectric layers

10	20	30	40
ELEM	VOLT1	VOLT2	VOLT_NP

Variables:

ELEM	Element number
VOLT1	Applied voltage to layer #1
VOLT2	Applied voltage to layer #2
VOLT_NP	Applied voltage to layer #n_p

APPENDIX
TWO

POST-PROCESSING PROGRAM

The results output file written from PROTEC for post-processing with PATRAN is called PATRAN.INP and here, a program called PRO-PAT translates the PATRAN.INP file into various output files such as the static displacements, element voltages for piezoelectric analysis and modal displacement solutions.

The PRO-PAT.F program is menu driven and it requires user interaction in order to decide if the translation is for nodal or element data.